การออกแบบตัวชดเชยสำหรับระบบไฟฟ้ากำลังที่ปฏิบัติการ
ภายใต้การกระเพื่อมของแรงดันโหลดซึ่งสอดคล้องกับเงื่อนไขขอบเขต

นายกิตติชัย แซ่เตีย

วิทยานิพนธ์นี้เป็นส่วนหนึ่งของการศึกษาตามหลักสูตรปริญญาวิศวกรรมศาสตรมหาบัณฑิต
สาขาวิชาวิศวกรรมไฟฟ้า ภาควิชาวิศวกรรมไฟฟ้า
คณะวิศวกรรมศาสตร์ จุฬาลงกรณ์มหาวิทยาลัย
ปีการศึกษา 2551

DESIGN OF COMPENSATORS FOR POWER SYSTEMS OPERATING UNDER LOAD VOLTAGE FLUCTUATION SATISFYING BOUNDING CONDITIONS

Mr. Kittichai Tia

A Thesis Submitted in Partial Fulfillment of the Requirements
for the Degree of Master of Engineering Program in Electrical Engineering
Department of Electrical Engineering
Faculty of Engineering
Chulalongkorn University
Academic Year 2008

Thesis Title	DESIGN OF COMPENSATORS FOR POWER SYSTEMS OPERATING UNDER LOAD VOLTAGE FLUCTUATION SATISFYING BOUNDING CONDITIONS
By	Mr. Kittichai Tia
Field of Study	Electrical Engineering
Advisor	Assistant Professor Suchin Arunsawatwong, Ph.D.
Co-Advisor	Professor Bundhit Eua-arporn, Ph.D.

Accepted by the Faculty of Engineering, Chulalongkorn University in Partial Fulfillment of the Requirements for the Master's Degree

.... Dean of the Faculty of Engineering
(Associate Professor Boonsom Lerdhirunwong, Dr. Ing.)

THESIS COMMITTEE

.... Chairman
(Associate Professor David Banjerdpongchai, Ph.D.)

.... Advisor
(Assistant Professor Suchin Arunsawatwong, Ph.D.)

.... Co-Advisor
(Professor Bundhit Eua-arporn, Ph.D.)

.... Examiner
(Naebboon Hoonchareon, Ph.D.)

.... External Examiner
(Associate Professsor Waree Kongprawechnon, Ph.D.)

กิตติชัย แซ่เตีย: การออกแบบตัวชดเชยสำหรับระบบไฟฟ้ากำลังที่ปฏิบัติการภายใต้การกระเพื่อมของแรงดันโหลดซึ่งสอดคล้องกับเงื่อนไขขอบเขต (DESIGN OF COMPENSATORS FOR POWER SYSTEMS OPERATING UNDER LOAD VOLTAGE FLUCTUATION SATISFYING BOUNDING CONDITIONS), อ. ที่ปรึกษาวิทยานิพนธ์หลัก: ผศ.ดร. สุชิน อรุณสวัสดิ์วงศ์, อ. ที่ปรึกษาวิทยานิพนธ์ร่วม: ศ.ดร. บัณฑิต เอื้ออาภรณ์, 40 หน้า.

ในการปฏิบัติการระบบไฟฟ้ากำลัง และ การควบคุมนั้น การเปลี่ยนแปลงของโหลดอย่างรุนแรง มีอิทธิพลอย่างมากต่อเสถียรภาพและสมรรถนะของระบบ เช่น มุมของโรเตอร์ แรงดันที่ขั้วเครื่องกำเนิดไฟฟ้า การเปลี่ยนแปลงความเร็วของโรเตอร์ และแรงดัน ของบัสที่อยู่ใกล้กับบัสของโหลดที่มีการเปลี่ยนแปลง วิทยานิพนธ์นี้นำเสนอการออกแบบตัวชดเชยสำหรับระบบไฟฟ้ากำลังที่อยู่ภายใต้การกระเพื่อมของแรงดันโหลด โดยใช้หลักการเข้าคู่และวิธีอสมการ สำหรับการออกแบบนี้ การเปลี่ยนแปลงของแรงดันโหลดทั้งหมด ที่เป็นไปได้ ถูกจำลองเป็นสัญญาณรบกวนคงอยู่ที่มีขอบเขตทั้งขนาด และการเปลี่ยนแปลงของขนาดมีค่าจำกัด วัตถุประสงค์หลักในการออกแบบคือทำให้แน่ใจว่า ขนาดของสัญญาณขาออกของระบบที่สนใจ จะไม่เบี่ยงเบนไปจากค่าที่ภาวะอยู่ตัวมากกว่าขอบเขตที่ยอมรับได้สำหรับทุกสัญญาณรบกวนที่เป็นไปได้ ตลอดช่วงเวลาที่พิจารณา การออกจากขอบเขตที่ยอมรับได้ของสมรรถนะของระบบ อาจทำให้เกิดความไม่เสถียรของระบบ และเหตุการณ์ที่ไม่สามารถยอมรับได้ตามมา เมื่อได้คำตอบของการออกแบบแล้ว ระบบไฟฟ้ากำลังจะปฏิบัติการ โดยมีสมรรถนะของระบบ อยู่ในขอบเขตที่ยอมรับได้ ตลอดช่วงเวลาที่พิจารณา ผลการจำลองเชิงเลขของระบบไฟฟ้ากำลังแสดงให้เห็นว่าทฤษฎีการออกแบบที่ใช้ในงานนี้เหมาะสมและมีประสิทธิภาพ ซึ่งทำให้การกำหนดรูปแบบปัญหาเป็นไปอย่างสมจริง

ภาควิชา วิศวกรรมไฟฟ้า	ลายมือชื่อนิสิต ....
สาขาวิชา วิศวกรรมไฟฟ้า	ลายมือชื่อ อ.ที่ปรึกษาวิทยานิพนธ์หลัก ....
ปีการศึกษา 2551	ลายมือชื่อ อ.ที่ปรึกษาวิทยานิพนธ์ร่วม ....

##507 05404 21: MAJOR ELECTRICAL ENGINEERING

KEYWORDS : DYNAMIC PERFORMANCE / COMPENSATION / LOAD VOLTAGE FLUCTUATION / CONTROL DESIGN / PRINCIPLE OF MATCHING / METHOD OF INEQUALITIES

KITTICHAI TIA: DESIGN OF COMPENSATORS FOR POWER SYSTEMS OPERATING UNDER LOAD VOLTAGE FLUCTUATION SATISFYING BOUNDING CONDITIONS. ADVISOR: ASST. PROF. SUCHIN ARUNSAWATWONG, Ph.D., CO-ADVISOR: PROF. BUNDHIT EUA-ARPORN, Ph.D., 40 pp.

In power system operation and control, large load variation greatly influences the system's stability and the dynamic performances such as the rotor angle, the terminal voltage, the speed deviation of the generator, and the voltages of nearby buses. This thesis presents the design of compensators for power systems subject to random load voltage fluctuation by using the principle of matching and the method of inequalities. In the design, all possible load voltage variations are treated as persistent disturbances having uniform bounds on the magnitude and the slope. The principal design objective is to ensure that the magnitudes of the outputs of interest do not deviate from their nominal values more than the allowable bounds for all time in the presence of all the possible disturbances. Any violation of the bounds may cause the system's instability and unacceptable consequences. Once a solution is found, the system is guaranteed to operate satisfactorily for all time. The numerical results demonstrate that the framework adopted here is suitable and effective, thereby giving a realistic formulation of the design problem.

Department:	Electrical Engineering	**Student's Signature**	กิตติชัย แซ่เตีย
Field of Study:	Electrical Engineering	**Advisor's Signature**	S. Arunsawatwong
Academic Year	2008	**Co-Advisor's Signature**	B. Eua-arporn

Acknowledgments

I would like to express my profound gratitude to my principal advisor, Assistant Professor Suchin Arunsawatwong, for his constant guidance, helpful advice, and encouragement since I was an undergraduate student. Grateful acknowledgment is also made to my co-advisor, Professor Bundhit Eua-arporn, for his constructive suggestions on the power system used in my research.

I would like to thank Associate Professor David Banjerdpongchai for providing me with the necessary background on control system theory and kindly serving on the thesis committee as a chairman. I am thankful to Dr. Naebboon Hoonchareon for introducing me to the field of power system's dynamic and stability, for his fruitful comments on my work, and for being one of the committees of this thesis. I am also grateful to Associate Professor Waree Kongprawechnon for her willingness to serve on the thesis committee.

I gratefully acknowledge Chulalongkorn University Scholarship of the Honor Graduate Program for Electrical Engineering Students for the full financial support throughout my master's study. Many thanks are due to colleagues who had given technical helps while this research was ongoing. In particular, I would like to thank Warit Silpsrikul for useful discussions regarding the computation of the peak outputs and package "SeDuMi".

Last but not least, I would like to thank my family for their understanding and kind support during my study. Thanks are also given to all members of Control Systems Research Laboratory, Chulalongkorn University for their encouragement and friendship.

Contents

List of Tables

List of Figures

List of Notations

Symbols

$\mathcal{P}$	The possible input set
α	The spectral abcissa
$\hat{y}_i$	The ith peak output of the system
$\tilde{y}_i$	The ith convenient upper bound of $\hat{y}_i$
I_{MN}	An integral operator (see the definition in [11])

Acronyms

PSS	Power System Stabilizer
SVC	Static Var Compensator
PoM	Principle of Matching
MoI	Method of Inequalities
MBP	Moving Boundaries Process

CHAPTER I

INTRODUCTION

1.1 Research Motivation

In power system operation and control, it is widely known (see, e.g., [1–6]) that large load variation greatly influences the system's stability and dynamic performances. In designing a compensator so as to improve the stability and the dynamic performances, the load characteristics should be taken into account.

More specifically, the fluctuation of the load has an impact on the rotor angle, the terminal voltage, the speed deviation of the generator, and the voltages of the nearby buses. For example, the operation of an electric arc furnace causes the fluctuation of load voltage in the power system and can significantly deteriorate the stability and the performances of a nearby generating unit. In order to keep the system in stable operation with satisfactory performances, it is necessary that the outputs of interest be kept within their prescribed bounds in the presence of load voltage fluctuation. Any violation of these bounds can give rise to the system instability and, consequently, may cause blackout in widespread area.

In this connection, the improvement of the power system's stability and performances can be carried out by utilizing devices such as Power System Stabilizer (PSS), Static Compensator (STATCOM), Static VAR Compensator (SVC) and Super Conducting Magnetic Energy Storage (SMES). When the system is subject to the load that fluctuates all the times (within a reasonably large range), the problem of tuning parameters for these compensation devices is not easy to solve.

Most of available control theories are based on properties defined in terms of the system outputs in response to certain deterministic test inputs (e.g., the unit-step function). When the load has uncertain characteristics, such control theories no longer provide effective tools for compensating the power system. This is mainly because the design problem is not formulated in a realistic manner. For this reason, to arrive at an accurate and realistic formulation, the design problem should take into account the characteristics of the input (which is the fluctuating behavior of the load).

1.2 Literature Review

There have been many researches on how to improve the dynamic performances of power systems subject to load voltage fluctuation. Some of them are as follows.

- Wu *et al* [1, 2] propose the improvement of dynamic performances of synchronous generators near electric arc furnace loads. They employ the step response criterion for determining the adjustable parameters of the static excitation system.

- Chen *et al* [3] investigate the voltage fluctuation problem of a large steel plant. They compensate the power system by using adaptive control of exciter and governor of the cogenerator.

- Sensarma *et al* [5] make use of STATCOM for compensating the power system. The design method used is based on frequency domain analysis. They perform simulations of compensated power systems with the test input being the step change in voltage reference.

- Zhao and Jiang [6] present the use of SVC for improving the performances of the power system. The design parameters of SVC are determined by using the robust optimization techniques. After obtaining the design parameters, a fault in the transmission line applies to the power system so as to test the performances of the compensated system.

- Tay and Conlon [7] describe how to use an SMES in compensating the fluctuation of the load. They assume that the SMES is connected in parallel with the disturbing loads. The SMES compensates the power system by providing the active and reactive power for the fluctuating load. The compensation is carried out by using optimization strategy.

- Sakamoto *et al* [8] study the development of Superconducting Generator (SCG) for mitigation of the voltage fluctuation in power systems with a wind power generator. The operational impedance-based method, see the references therein for details, is adopted for obtaining the mathematical model of SCG. After that, they demonstrate the effectiveness of SCG by performing simulations of the operation of the wind generator equipped with SCG.

Apparently, no one has considered the uncertain characteristics of the load fluctuation. Evidently, the design formulations employed by those researchers are not realistic in practice. For example, the system responses to a step input cannot be used to accurately describe the performance of the system subject to the load voltage fluctuating randomly. To assess the actual performance of the system, design engineers may have to perform simulations with a number of possible load waveforms after obtaining a design result, so as to check whether the system can performs satisfactorily or not. This usually involves repeated redesign and simulation of performances, a process that can be very time-consuming.

1.3 Thesis Objective

The objective of this thesis is to design a compensator for improving the stability and the dynamic performance of a power system operating under load fluctuation, in which all possible load voltage variations are modelled as persistent functions satisfying certain norm-bounding conditions (see (2.3)). As a result, the system's stability and performances are guaranteed to be maintained within their acceptable ranges as long as the load voltage variation satisfies the bounding conditions.

The design methodology adopted in this work is an adjunct to Zakian's framework [15], which comprises the principle of matching [14] and the method of inequalities [10, 12]. The principle of matching suggests what kind of design criteria should be used so that the design problem is formulated in an accurate and realistic manner, whereas the method of inequalities requires that the design problem be cast as a set of inequalities that can be solved in practice.

In this thesis, in order to illustrate how the framework can be used in improving the system's stability and performances, the compensation will be carried out by using PSS and SVC. However, it is important to note that the framework adopted here is not only applicable to the design of PSS and SVC but also the design of other types of compensator.

1.4 Scope of Thesis

1. The model of power systems used in this research is based on the model of a single machine connecting to an infinite bus.
2. The linearized model is used for designing compensators for power systems.
3. Load voltage fluctuation is modelled as persistent functions having uniform bounds on magnitude and derivative.

1.5 Methodology

1. Collect and study literature on the design of compensators for improving the dynamic performances of power systems subject to load voltage fluctuation.
2. Formulate the design problem such that the design objectives are in the form of inequalities and the voltage of the load satisfies bounding norm conditions.
3. Employ the principle of mathcing and the method of inequalites to the design problem.

1.6 Contributions

1. A method for designing compensators for improving dynamic performances of a power system which operates under load voltage fluctuation
2. A case study of compensation of a single machine power system subject to load voltage fluctuation which can be extended to the case of multi-machine power systems.

1.7 Structure of Thesis

The organization of the thesis is as follows. In the next chapter, the fundamental design theory is explained. Chapter 3 presents the improvement of the power system's stability and performances by using PSS. Chapter 4 describes the enhancement of the power system's stability and perfomances by using SVC. In the last chapter, conclusions are given.

CHAPTER II

FUNDAMENTAL DESIGN THEORY

In this chapter, an overview of the fundamental theory used in designing compensators of power systems is described.

Consider a linear, time-invariant and causal system whose input $f : \mathbb{R} \to \mathbb{R}$ and outputs $y_i : \mathbb{R} \to \mathbb{R}$ are related by the convolution integral

$$y_i(t, f) = \int_{-\infty}^{t} h^i(t - \tau) f(\tau) d\tau \quad (i = 1, 2, \ldots, m), \tag{2.1}$$

where $h^i : \mathbb{R} \to \mathbb{R}$ denotes the impulse response of y_i, and $h^i(t) = 0 \; \forall t < 0$. In this work, suppose that

$$h^i(t) = \beta_i \delta(t) + h_1^i(t), \tag{2.2}$$

where β_i is a real number, δ denotes Dirac delta function and $h_1^i : \mathbb{R} \to \mathbb{R}$ is bounded and piecewise continous.

Assume that the input $f : \mathbb{R} \to \mathbb{R}$ is known only to the extent that it belongs to the set $\mathcal{P}$ described by

$$\mathcal{P} \triangleq \{f : \|f\|_\infty \leq \mathcal{M}, \|\dot{f}\|_\infty \leq \mathcal{D}\}, \tag{2.3}$$

where $\mathcal{M}$ and $\mathcal{D}$ are some positive numbers. The set $\mathcal{P}$, called the possible set, contains all the inputs that happen or can happen or are likely to happen in practice.

A chief design objective is to ensure that the outputs y_i remain within prescribed bounds in the presence of disturbance acting to the system. That is to say,

$$|y_i(t, f)| \leq \varepsilon_i \quad \forall t \, \forall f \quad (i = 1, 2, \ldots, m), \tag{2.4}$$

where $y_i(t, f)$ denote the value of outputs y_i in response to a possible input f at time t and ε_i are the largest values of y_i that can be accepted. Notice that the crieria (2.4) are not computationally tractable.

Define

$$\hat{y}_i \triangleq \sup_{f \in \mathcal{P}} \sup_{t \geq 0} |y_i(t, f)| \quad (i = 1, 2, \ldots, m), \tag{2.5}$$

where the performance measures $\hat{y}_i$ are sometimes called the peak outputs for the possible set $\mathcal{P}$. It is easy to see that the condition (2.4) is equivalent to

$$\hat{y}_i \leq \varepsilon_i \quad (i = 1, 2, \ldots, m). \tag{2.6}$$

Consequently, the inequalities (2.6) become practical conditions only if the peak outputs $\hat{y}$ are computable.

2.1 Computation of Performance Measures

It is shown [9, 16] that the problem of computing $\hat{y}_i$ for (2.1) can be rewritten as

$$\hat{y}_i = \sup\{J_i(f) : f \in \mathcal{P}\}, \tag{2.7}$$

where $J_i(f)$ is the cost function given by

$$J_i(f) = \int_{-\infty}^{\infty} h^i(-\tau) f(\tau) d\tau. \tag{2.8}$$

It is shown [16] that if the system is BIBO stable, then the improper integral in (2.8) is well approximated as

$$J_i(f) \approx \beta_i f(0) + \int_{-T}^{T} h_1^i(-\tau) f(\tau) d\tau, \quad T > 0 \tag{2.9}$$

for a sufficiently large T. From (2.9), one can easily compute $J_i(f)$ using finite difference approximation schemes.

2.1.1 Cost Function Approximation

For $t \in [-T, T]$, the trajectories $h_1^i(t)$ and $f(t)$ are represented by the vectors $\bar{h}^i \in \mathbb{R}^{2n+1}$ and $\bar{f} \in \mathbb{R}^{2n}$ such that

$$\bar{h}^i \triangleq \left[h_{-n}^i, h_{-n+1}^i, \ldots, h_{n-1}^i, h_n^i\right]^T \tag{2.10}$$

and

$$\bar{f} \triangleq \left[f_{-n}, f_{-n+1}, f_{-n+2}, \ldots, f_{n-1}, f_n\right]^T, \tag{2.11}$$

where $h_k^i = h_1^i(t_k)$ and $f_k = f(t_k)$. The time point t_k is given by

$$\begin{aligned} t_{-n} &= T, \\ t_{k+1} &= t_k + \sigma \quad \text{for} \quad i = -n, -n+1, \ldots, n-1, \end{aligned}$$

where the uniform difference $\sigma = T/n$ is used.

It is important to note that the optimization in (2.7) is convex and that there are more than one maximal inputs (i.e., the inputs that give the peak output). In order to make the maximal inputs obtained from solving (2.7) unique, it is necessary to set up $f_{-n} = 0$ (see [16] for details). Hence, (2.11) is rewritten as

$$\bar{f} \triangleq \left[0, f_{-n+1}, f_{-n+2}, \ldots, f_{n-1}, f_n\right]^T. \tag{2.12}$$

Next, we use Simpson's rule in approximating the truncated integral in (2.8). If the positive number n is chosen to be even, then we have

$$J_i(f) \approx \mathbf{c}_i^T \bar{f} \triangleq \mathbb{J}_i(\bar{f}), \tag{2.13}$$

where the vector $\mathbf{c}_i \in \mathbb{R}^{2n}$ in (2.13) is given by

$$\mathbf{c}_i = \frac{\sigma}{3}\left[4h_{n-1}^i, 2h_{n-2}^i, \ldots, 4h_{-1}^i, \frac{3\beta_i}{\sigma} + h_0^i, 0_{1\times n}\right]^T. \tag{2.14}$$

2.1.2 Constraints Approximation

Let $x \preceq y$ denote componentwise inequality between vectors x and y. The inequality $\|f\|_\infty \leq \mathcal{M}$ can be replaced by

$$\mathbf{I}\bar{f} \preceq \mathcal{M}\bar{\mathbf{1}} \quad \text{and} \quad -\mathbf{I}\bar{f} \preceq \mathcal{M}\bar{\mathbf{1}}, \tag{2.15}$$

where $\mathbf{I}$ and $\bar{\mathbf{1}}$ denote the identity matrix and a vector with all components being one, respectively. Similarly, the inequality $\|\dot{f}\|_\infty \leq \mathcal{D}$ can be rewritten as

$$Q_d\bar{f} \preceq \mathcal{D}\bar{\mathbf{1}} \quad \text{and} \quad -Q_d\bar{f} \preceq \mathcal{D}\bar{\mathbf{1}}. \tag{2.16}$$

where $Q_d \in \mathbb{R}^{2n\times 2n}$ is the matrix used in approximating the derivative by first-order forward difference formula

$$Q_d = \frac{1}{\sigma}\begin{bmatrix} 1 & 0 & 0 & \dots & 0 & 0 & 0 \\ -1 & 1 & 0 & \dots & 0 & 0 & 0 \\ 0 & -1 & 1 & \dots & 0 & 0 & 0 \\ \vdots & \vdots & \vdots & \ddots & \vdots & \vdots & \vdots \\ 0 & 0 & 0 & \dots & -1 & 1 & 0 \\ 0 & 0 & 0 & \dots & 0 & -1 & 1 \end{bmatrix}.$$

Accordingly, an approximant of $\hat{y}_i$ is the solution of the following large-scale optimization problem

$$\hat{y}_i \cong \max\{\mathbb{J}_i(\bar{f}) : \bar{f} \text{ satisfies (2.15) and (2.16)}\}. \tag{2.17}$$

The optimization problem in (2.17) has two important properties. First, it is shown in [16] that when both Simpson's rule and the first order forward difference formula are used, the problem (2.17) is convex for any difference $\sigma > 0$. Second, the matrices associated with (2.17) are sparse.

Nowadays, large-scale convex optimization problems can readily be solved by efficient numerical algorithms. Therefore, (2.17) can be solved efficiently in practice for any value of $\sigma > 0$ used. In this work, we use the package called "SeDuMi" [17] to solve the convex optimization problem (2.17).

2.2 Convenient Upper Bounds of the Peak Outputs

Note that the calculation of $\hat{y}_i$ is sophisticated. Thus, for simplicity in demonstrating the idea and the usefulness of the design framework, one may consider using conveniet upper bounds $\tilde{y}$ of $\hat{y}_i$ (i.e. $\tilde{y}_i \geq \hat{y}_i$) given by

$$\tilde{y}_i = |s_{i,ss}|\, M + \|s_i - s_{i,ss}\|_1\, D, \tag{2.18}$$

where s_i are the responses y_i due to the unit step input $\mathbf{1}$ (i.e., $s_i(t) = y_i(t, \mathbf{1})$) and $s_{i,ss}$ denotes the steady-state values of s_i. See [14] for the derivation of formula (2.18).

2.3 Stabilization of Performance Measures

Let $p \in \mathbb{R}^n$ denote a vector of design parameters. In solving the inequalities

$$\tilde{y}_i(p) \leq \varepsilon_i \quad (i = 1, 2, \dots, m) \tag{2.19}$$

by numerical methods, it is necessary to obtain a stability point—that is, a point $p \in \mathbb{R}^n$ such that

$$\tilde{y}_i(p) < \infty \ \ \forall i. \tag{2.20}$$

This is because search algorithms, in general, are able to seek a solution of (2.20) only if they start from such a point (see [13, 15] for the details). In order to formulate the problem of determining a stability point so that it is suitable for solution by numerical method, it is necessary to replace (2.20) by an equivalent statement that is soluble by numerical methods.

Assume that a state-space realization of the system is $\{A, B, C, D\}$. Then one can easily prove that $\tilde{y}_i(p) < \infty$ for all i if all the eigenvalues of A lie in the open left half of the complex plane; that is to say, if

$$\alpha(p) < 0, \tag{2.21}$$

where $\alpha(p)$ is called the spectral abscissa of A and given by

$$\alpha(p) \triangleq \max_i \{\text{Re } \lambda_i(A)\} \tag{2.22}$$

and $\lambda_i(A)$ denotes an eigenvalues of A. Notice that $\alpha(p) < \infty$ for all values of $p \in \mathbb{R}^n$ and that α can be computed economically in practice. Accordingly, the inequality (2.21) is always soluble by numerical methods [10], [14], [13].

CHAPTER III

ENHANCEMENT OF POWER SYSTEM'S STABILITY AND PERFORMANCES BY USING PSS

This chapter describes the enhancement of stability and performances of power system operating under load voltage fluctuation by using PSS in the excitation system of the generator.

3.1 Power System Model

The power system model used in this study is taken from [4], which is a standard textbook, and is modified by adding a local load at bus 2. The system consists of a transmission network, a generator, an excitation system and a governor control loop. Each of them will be modelled individually and thereafter grouped as an interconnected system.

The single line diagram of the system is shown in Figure 3.1, where i_T denotes the generator current, e_T the terminal voltage of the generator, e_B the voltage at the infinite bus, v_L the load voltage, L_{tr} an inductance of a tranformer connecting the generator to bus 2 and L_l an inductance of the transmission line connecting bus 2 to the infinite bus.

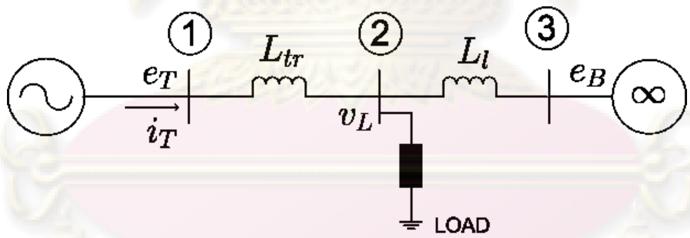

Figure 3.1: Power system model under varying load voltage conditions

3.1.1 The Transmission Network Model

Assume that the power system operates under three-phase balanced condition. The transmission network model is derived from the equivalent circuit of the single-line diagram shown in Figure 3.1.

From the equivalent circuit (in the abc reference frame) shown in Figure 3.2, one easily obtains

$$e_T = L_{tr}\frac{di_T}{dt} + v_L, \tag{3.1}$$

where

$$\left.\begin{array}{rcl} e_T(t) & = & E_T(t)\sin(\omega t + \varphi_1) \\ v_L(t) & = & V_L(t)\sin(\omega t + \varphi_2) \\ i_T(t) & = & I_T(t)\sin(\omega t + \varphi_3) \end{array}\right\}, \tag{3.2}$$

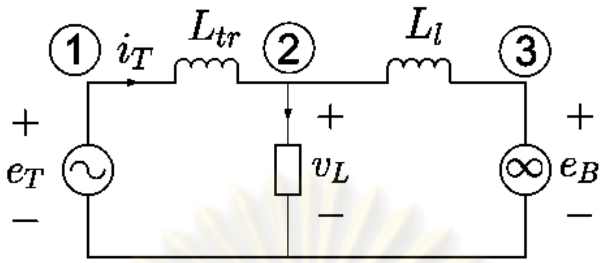

Figure 3.2: Equivalent circuit of single-line diagram of power system

and φ_i $(i = 1, 2, 3)$ are the phase angles of e_T, v_L and i_T at the steady state.

In the following, the network variables in the abc reference frame will be transformed into the dqo reference frame (see, for example, [4] for the details). By using such a transformation, the mathematical model of the system with the dqo variables is described by time-invariant differential equations, as opposed to time-varying differential equations in the abc reference frame. See Appendix A for details.

It is easy to verify that the transmission network is described by

$$\left.\begin{array}{rcl} \frac{dI_{T,d}}{dt} & = & \frac{1}{L_{tr}}(E_{T,d} - V_{L,d}) + \omega I_{T,q} \\ \frac{dI_{T,q}}{dt} & = & \frac{1}{L_{tr}}(E_{T,q} - V_{L,q}) - \omega I_{T,d} \end{array}\right\}, \tag{3.3}$$

where ($I_{T,d}$, $V_{L,d}$, $E_{T,d}$) and ($I_{T,q}$, $V_{L,q}$, $E_{T,q}$) are the d- and q-components of (I_T, V_L, E_T), respectively and the voltage magnitude in the abc reference frame is related to the voltage magnitude in the dqo reference frame by

$$\left.\begin{array}{rcl} I_T(t) & = & \sqrt{I_{T,d}^2(t) + I_{T,q}^2(t)} \\ V_L(t) & = & \sqrt{V_{L,d}^2(t) + V_{L,q}^2(t)} \\ E_T(t) & = & \sqrt{E_{T,d}^2(t) + E_{T,q}^2(t)} \end{array}\right\}. \tag{3.4}$$

3.1.2 The Synchronous Generator Model

The nonlinear mathematical model of a synchronous generator, expressed in terms of d- and q-flux linkages [4], is given by the following equations:

$$\left.\begin{array}{rcl} \frac{dE_q'}{dt} & = & \frac{1}{T_{do}'}(-E_q' + (X_d - X_d')I_{T,d} + E_{\mathrm{fd}}) \\ \frac{dE_d'}{dt} & = & \frac{1}{T_{qo}'}(-E_d' + (X_q - X_q')I_{T,q}) \\ \frac{d\delta}{dt} & = & \omega_b(\omega - \omega_s) = \omega_b \Delta\omega \\ \frac{d\Delta\omega}{dt} & = & \frac{1}{2H}(T_m - T_e - K_D \Delta\omega) \\ T_e & = & E_d' I_{T,d} + E_q' I_{T,q} + (X_q' - X_d') I_{T,d} I_{T,q} \end{array}\right\}, \tag{3.5}$$

where E_d' and E_q' are the transient electromotive forces, T_{do}' and T_{qo}' are the open circuit field time constants, X_d and X_q are the reactances, X_d' and X_q' are the transient reactances, E_{fd} is the field voltage, δ is the rotor angle of the generator, ω is the angular speed of the generator, H is the inerita constant, T_m is the mechanical input torque, T_e is the electrical input torque and K_D is the damping coefficient of the generator.

3.1.3 The Excitation System Model

The excitation system comprises a voltage transducer, an automatic voltage regulator (AVR) and a power system stabilizer (PSS). The block diagram of the excitation system is given in Figure 3.3 and its state-space representation is

$$\left.\begin{aligned} \frac{dv_1}{dt} &= \frac{1}{T_R}(E_T - v_1) \\ \frac{dv_2}{dt} &= K_s\frac{d\Delta\omega}{dt} - \frac{1}{T_W}v_2 \\ \frac{dv_3}{dt} &= \frac{1}{T_2}(T_1\frac{dv_2}{dt} + v_2 - v_3) \\ \frac{dv_4}{dt} &= \frac{1}{T_4}(T_3\frac{dv_3}{dt} + v_3 - v_4) \\ E_{\text{fd}} &= K_A(V_{\text{ref}} - v_1 + v_s). \end{aligned}\right\}, \tag{3.6}$$

where v_i and T_i $(i = 1, \ldots, 4)$ denote, respectively, the state variables and the lead-lag time constants of the excitation system, T_R is the transducer time constant, T_W is the washout time constant, K_s is the PSS gain, and v_s is the output signal of the PSS described by

$$v_s = \begin{cases} v_s^{\text{min}}, & v_4 < v_s^{\text{min}}, \\ v_4, & v_s^{\text{min}} \le v_4 \le v_s^{\text{max}}, \\ v_s^{\text{max}}, & v_4 > v_s^{\text{max}}. \end{cases} \tag{3.7}$$

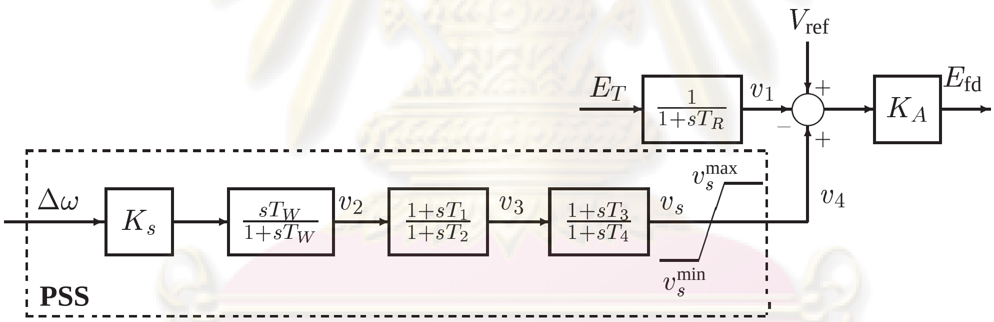

Figure 3.3: Block diagram of excitation system

It is worth noting that, in order to ensure that the PSS model always operates in the linear range, the stabilizer control signal v_s needs to satisfy

$$v_s^{\text{min}} \le v_s \le v_s^{\text{max}}, \tag{3.8}$$

where v_s^{min} and v_s^{max} are some constants.

3.1.4 The Governor Control Model

Figure 3.4 shows the block diagram of the governor control loop. The differential equations describing this subsystem are given by

$$\left.\begin{aligned} \frac{dg_1}{dt} &= \frac{K_I}{R}\Delta\omega \\ \frac{dg_2}{dt} &= \frac{1}{T_G}(\frac{\Delta\omega}{R} + g_1 - g_2) \\ \frac{dg_3}{dt} &= \frac{1}{T_P}(g_2 - g_3) \\ T_m &= T_{\text{ref}} - g_3 \end{aligned}\right\}, \tag{3.9}$$

where g_i $(i = 1, 2, 3)$ are the state variables, K_I is the integrator gain, R is the droop constant, T_G is the governor time constant, and T_P is the prime mover time constant.

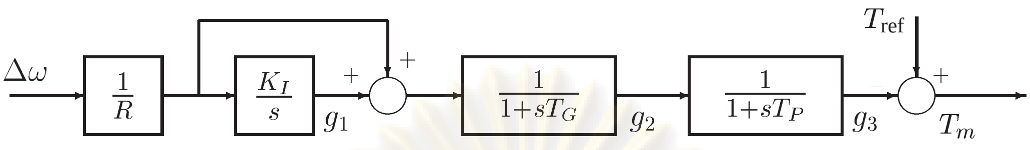

Figure 3.4: Block diagram of governor loop

3.1.5 The Interconnected Power System Model

On combining (4.3), (3.3), (4.4), and (4.6), the interconnected power system is therefore described by the following nonlinear differential equations

$$\frac{dx}{dt} = Tx + N(x,u) + Eu, \tag{3.10}$$

where $T \in \mathbb{R}^{13\times 13}$ and $E \in \mathbb{R}^{13\times 4}$ are constant matrices given in Appendix B. The state vector $x : \mathbb{R} \to \mathbb{R}^{13}$, the input vector $u : \mathbb{R} \to \mathbb{R}^{4}$ and the vector $N : \mathbb{R}^{13} \times \mathbb{R}^{4} \to \mathbb{R}^{13}$ and are given by

$$\begin{aligned}
x &= \begin{bmatrix} \delta & \Delta\omega & E'_q & E'_d & I_{T,d} & I_{T,q} & v_1 & v_2 & v_3 & v_4 & g_1 & g_2 & g_3 \end{bmatrix}^T, \\
N &= \begin{bmatrix} 0 & n_2 & 0 & 0 & n_5 & n_6 & n_7 & n_8 & n_9 & n_{10} & 0 & 0 & 0 \end{bmatrix}^T, \\
u &= \begin{bmatrix} V_{\text{ref}} & T_{\text{ref}} & V_{L,d} & V_{L,q} \end{bmatrix}^T,
\end{aligned}$$

where the nonzero elements of N are as follows:

$$\begin{aligned}
n_2 &= -\tfrac{1}{2H}(E'_d I_{T,d} + E'_q I_{T,q} + (X'_q - X'_d) I_{T,d} I_{T,q}), \\
n_5 &= \Delta\omega I_{T,q}, \\
n_6 &= -\Delta\omega I_{T,d}, \\
n_7 &= \tfrac{1}{T_R}\sqrt{E^2_{T,d} + E^2_{T,q}}, \\
n_8 &= -\tfrac{K_s}{2H}(E'_d I_{T,d} + E'_q I_{T,q} + (X'_q - X'_d) I_{T,d} I_{T,q}), \\
n_9 &= -\tfrac{K_s T_1}{2HT_2}(E'_d I_{T,d} + E'_q I_{T,q} + (X'_q - X'_d) I_{T,d} I_{T,q}), \\
n_{10} &= -\tfrac{K_s T_1 T_3}{2HT_2 T_4}(E'_d I_{T,d} + E'_q I_{T,q} + (X'_q - X'_d) I_{T,d} I_{T,q}).
\end{aligned}$$

By defining as an output vector y as

$$y = [\delta \quad E_T \quad \Delta\omega \quad v_s]^T,$$

the output equation of the interconnected system is described by

$$y = Sx + M(x,u), \tag{3.11}$$

where S and M are given by

$$S = \begin{bmatrix} 1 & 0 & 0 & 0 & 0 & 0 & 0 & 0 & 0 & 0 & 0 & 0 & 0 \\ 0 & 0 & 0 & 0 & 0 & 0 & 0 & 0 & 0 & 0 & 0 & 0 & 0 \\ 0 & 1 & 0 & 0 & 0 & 0 & 0 & 0 & 0 & 0 & 0 & 0 & 0 \\ 0 & 0 & 0 & 0 & 0 & 0 & 0 & 0 & 0 & 1 & 0 & 0 & 0 \end{bmatrix},$$

$$M = \begin{bmatrix} 0 & \sqrt{E_{T,d}^2 + E_{T,q}^2} & 0 & 0 \end{bmatrix}^T.$$

The generator parameters (in per unit with respect to 2220 MVA base) are shown in Tab. 4.1, and the power system is in the steady state with the following conditions:

$$P_o = 0.9 \text{ pu}, \quad Q_o = 0.436 \text{ pu} \quad \text{and} \quad E_{To} = 1.0 \text{ pu}.$$

By applying the steady-state analysis given in [4], one obtains a nominal operating point

$$x_o = \begin{bmatrix} \delta_o & \Delta\omega_o & E'_{qo} & E'_{do} & I_{T,do} & I_{T,qo} & v_{1o} & v_{2o} & v_{3o} & v_{4o} & g_{1o} & g_{2o} & g_{3o} \end{bmatrix}^T, \tag{3.12}$$

where $\delta_o = 69.9°$, $E'_{qo} = 1.024$ pu, $E'_{do} = 0.422$ pu, $I_{T,do} = 0.925$ pu, $I_{T,qo} = 0.380$ pu and others are zero.

Linearizing (3.10) and (3.11) about the operating point (3.12) yields

$$\left.\begin{aligned} \frac{d\Delta x}{dt} &= A\Delta x + B\Delta u \\ \Delta y &= C\Delta x + D\Delta u \end{aligned}\right\}, \tag{3.13}$$

where A, B, C and D are constant matrices given in Appendix B. Since V_{ref} and T_{ref} are constant, the incremental inputs in Δu are $\Delta V_{L,d}$ and $\Delta V_{L,q}$.

Table 3.1: Generator parameters in per unit base

K_D	=	10	H	=	3.5 sec	K_A	=	100
K_I	=	6.5	L_{tr}	=	0.15 pu	L_{l_1}	=	0.5 pu
L_{l_2}	=	0.93 pu	T'_{do}	=	8.0 sec	T'_{qo}	=	1.0 sec
T_G	=	0.2 sec	T_P	=	0.3 sec	T_R	=	0.015 sec
R	=	0.05	R_s	=	0.003 pu	X_d	=	1.81 pu
X_q	=	1.76 pu	X'_d	=	0.30 pu	X'_q	=	0.65 pu

3.2 Characterization of the Possible Set

This section describes how to characterize the possible set P, which contains all the possible load voltage deviations in the power system. From the previous section, one can see that the (incremental) inputs in the linearized model consists of $\Delta V_{L,d}$ and $\Delta V_{L,q}$, which are the d- and q-components of the load voltage deviation ΔV_L.

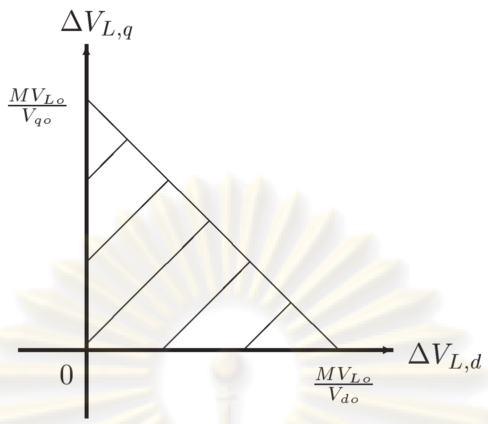

Figure 3.5: Region of possible $\Delta V_{L,d}$ and $\Delta V_{L,q}$ satisfying (3.19)

Assume that the power system is in the steady state for $t \le 0$ and the load voltage changes for $t > 0$. That is,

$$v_L(t) = \left\{ \begin{array}{cc} V_{Lo}\sin(\omega t + \varphi_2), & t \le 0 \\ V_{Lo}\sin(\omega t + \varphi_2) + \Delta v_L(t), & t > 0 \end{array} \right\}, \tag{3.14}$$

where V_{Lo} is constant and φ_2 is the phase angle of v_L at the steady state (see (4.1)). The term Δv_L is viewed as the disturbance to the power system and is written as

$$\Delta v_L(t) = \Delta V_L(t)\sin(\omega t + \varphi_2) \;\text{ for }\; t > 0. \tag{3.15}$$

In practice, the deviation of the load voltage $\Delta v_L(t)$ is bounded by some positive value. That is to say,

$$|\Delta v_L(t)| \le \mathcal{M} \quad \forall t \ge 0, \tag{3.16}$$

where M is a positive constant. According to (3.15), it readily follows that

$$|\Delta V_L(t)| \le \mathcal{M}. \tag{3.17}$$

Let V_{do} and V_{qo} denote the d- and q-components of V_{Lo}, which can be obtained in the linearization of (3.10). Using (3.17), one obtains

$$\left| \sqrt{(\Delta V_{L,d} + V_{do})^2 + (\Delta V_{L,q} + V_{qo})^2} - V_{Lo} \right| \le \mathcal{M}. \tag{3.18}$$

Normally, the load voltage deviates about 1–5% from its nominal value. This is to say, the bound M is much smaller than V_{Lo}. Hence, the terms $\mathcal{M}^2$, $\Delta V_{L,d}^2$ and $\Delta V_{L,q}^2$ are sufficiently small to be neglected in the calculation. The inequality (3.18) can be therefore simplified as

$$\Delta V_{L,d} V_{do} + \Delta V_{L,q} V_{qo} \le \mathcal{M} V_{Lo}. \tag{3.19}$$

Figure 3.5 shows the region in which the load voltage deviations $\Delta V_{L,d}$ and $\Delta V_{L,q}$ satisfy the condition (3.19). We can see that the possible maximum values of $\Delta V_{L,d}$ and $\Delta V_{L,q}$ are, respectively, $\frac{MV_{Lo}}{V_{do}}$ and $\frac{MV_{Lo}}{V_{qo}}$. For simplicity, the bounding conditions used in this work are set to be equal by using the minimum value of $\left\{\frac{MV_{Lo}}{V_{do}}, \frac{MV_{Lo}}{V_{qo}}\right\}$. Accordingly, the possible input set $\mathcal{P}$ used in the subsequent design is defined as

$$\mathcal{P} \triangleq \left\{(\Delta V_{L,d}, \Delta V_{L,q}) : \begin{array}{ll} \|\Delta V_{L,d}\|_\infty \le \mathcal{M}_d, & \|\Delta \dot{V}_{L,d}\|_\infty \le \mathcal{D}_d, \\ \|\Delta V_{L,q}\|_\infty \le \mathcal{M}_q, & \|\Delta \dot{V}_{L,q}\|_\infty \le \mathcal{D}_q \end{array}\right\}, \tag{3.20}$$

where $\mathcal{M}_d$, $\mathcal{M}_q$, $\mathcal{D}_d$ and $\mathcal{D}_q$ are some positive numbers.

Since there are two components of disturbances ($\Delta V_{L,d}$ and $\Delta V_{L,q}$), The calculation of the upper bounds $\tilde{y}_i$ and $\hat{y}_i$ defined in (2.18) and (2.17) can be extended in a straightforward manner.

Using the properties of linear systems, it can be verified that

$$\tilde{y}_i = \left|s^d_{i,ss}\right| \mathcal{B}_d + \left\|s^d_i - s^d_{i,ss}\right\|_1 \mathcal{D}_d + \left|s^q_{i,ss}\right| \mathcal{B}_q + \left\|s^q_i - s^q_{i,ss}\right\|_1 \mathcal{D}_q, \tag{3.21}$$

where s^d_i denote the responses y_i when $\Delta V_{L,d} = \mathbf{1}$ and $\Delta V_{L,q} = 0$, and s^q_i denote the responses y_i when $\Delta V_{L,d} = 0$ and $\Delta V_{L,q} = \mathbf{1}$. and $(s^d_{i,ss}, s^q_{i,ss})$ denote the steady-state values of s^d_i and s^q_i, respectively.

It may be noted that $(s^d_{i,ss}, s^q_{i,ss})$ are computed by using the final value theorem, step responses are calculated by using Zakian's I_{MN} recursion [11] (which is economical and reliable even if the system is very stiff), and the one-norm is computed by using the trapezoidal rule of integration.

3.3 Design Formulation

In the subsequent design, a PSS is used as a case study for improving the performance of the power system, where the speed deviation of the generator $\Delta\omega$ is fedback to the PSS. The configuration of the feedback control system is shown in Figure 3.6.

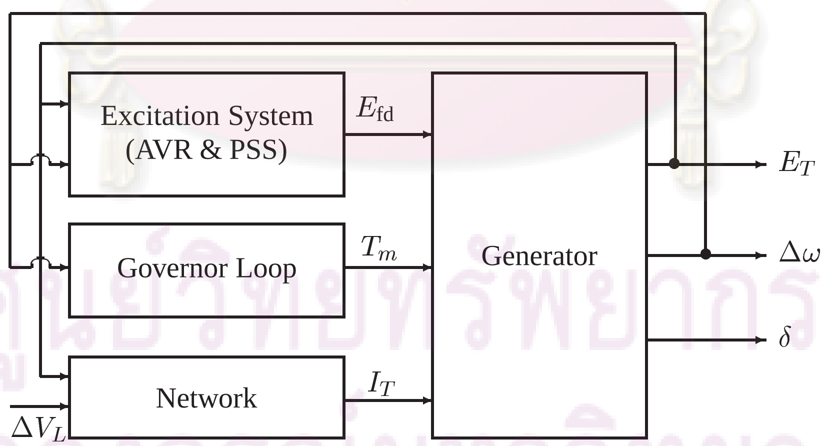

Figure 3.6: Configuration of the power system with certain outputs fedback to PSS

To ensure the good performances of the power system, the following requirements (which is based on a practical operating criteria [4]) should be taken into design consideration:

- the change of any generator's rotor angle should not be too high, for example, 55°–60°;

- the change of terminal voltage of the generator should be maintained within $\pm 3\%$ from its nominal value;
- the speed deviation of the generator should be restricted within ± 0.1 Hz from its nominal value;
- the control signal v_s should remain within the linear range of operation of ± 0.2 pu.

From the above requirements, the principal design specifications are expressed by the following set of inequalities:

$$\left.\begin{array}{lcccl} \phi_1(p) & \triangleq & \Delta\tilde{y}_1 & \leq & 55^\circ \\ \phi_2(p) & \triangleq & \Delta\tilde{y}_2 & \leq & 0.03 \text{ pu} \\ \phi_3(p) & \triangleq & \Delta\tilde{y}_3 & \leq & 0.002 \text{ pu} \\ \phi_4(p) & \triangleq & \Delta\tilde{y}_4 & \leq & 0.2 \text{ pu} \end{array}\right\}, \tag{3.22}$$

where $p \triangleq \begin{bmatrix} K_s & T_W & T_1 & T_2 & T_3 & T_4 \end{bmatrix}^T$ is the vector of design parameters in the PSS.

From the requirements in (3.22), it is clear that the design problem indeed has several objectives, as suggested by the method of inequalities. In this work, inequalities (3.22) are solved by a numerical search algorithm called the moving boundaries process (MBP). See [10, 15] for the details of the algorithm.

3.4 Numerical Results

This section presents the numerical results of the design problem formulated in Section . In this work, assume that the deviation of load voltage $\Delta V_{L,d}$ and $\Delta V_{L,q}$ is bounded by 0.05 pu of their nominal value and the rate of change is bounded by 0.02 pu/s. So, the bound $\mathcal{M}_d$, $\mathcal{M}_q$, $\mathcal{D}_d$ and $\mathcal{D}_q$ are given as follows:

$$\mathcal{M}_d = \mathcal{M}_q = 0.05 \text{ pu} \quad \text{and} \quad \mathcal{D}_d = \mathcal{D}_q = 0.02 \text{ pu/s}.$$

3.4.1 Design of PSS by Using the Upper Bounds of the Peak Outputs

In this subsection, we make use of the upper bounds of the peak outputs $\tilde{y}$ as performance measures. By using the MBP algorithm, the following design is obtained

$$p = \begin{bmatrix} 34.50 & 0.023 & 0.230 & 0.010 & 0.014 & 0.950 \end{bmatrix}^T,$$

and the corresponding performance measures are

$$\begin{array}{lcll} \phi_1 & = & 53.97^\circ & (\leq \ 55^\circ), \\ \phi_2 & = & 0.0272 \text{ pu} & (\leq \ 0.03 \text{ pu}), \\ \phi_3 & = & 0.0012 \text{ pu} & (\leq \ 0.002 \text{ pu}), \\ \phi_4 & = & 0.0154 \text{ pu} & (\leq \ 0.2 \text{ pu}). \end{array}$$

In the following simulation, suppose that the power system is in the steady state at the beginning and the disturbances apply to the power system. To verify the design results, a random test input is generated using the function **rand** in MATLAB (where the time interval used is one second) such that its magnitude and the magnitude of its slope are bounded by 0.05 pu and 0.02 pu/s, respectively. The waveform of random test inputs is shown in Figure 3.7.

The system's output responses to the test inputs are shown in Figure 3.8. Furthermore, it is found that the results so obtained agree with those obtained from the simulation of the actual nonlinear systems.

3.4.2 Design of PSS by Using the Peak Outputs

In this subsection, we use of the peak outputs $\hat{y}_i$ defined in chapter 2 as performance measures. By using the MBP algorithm, the satisfactory design parameters are the same as those obtained in the previous subsection and the corresponding performance measures are

$$\begin{array}{lllll} \phi_1 & = & 43.27^\circ & (\leq & 55^\circ), \\ \phi_2 & = & 0.0263 \text{ pu} & (\leq & 0.03 \text{ pu}), \\ \phi_3 & = & 0.0012 \text{ pu} & (\leq & 0.002 \text{ pu}), \\ \phi_4 & = & 0.0154 \text{ pu} & (\leq & 0.2 \text{ pu}). \end{array}$$

Table 3.2 shows the peak outputs of the system with the PSS' parameters obtained in the design by using the upper bounds of peak outputs as performance measures. Note that the value of peak outputs are less than or equal to thier upper bounds.

Accordingly, using the peak outputs $\hat{y}_i$ as performance measures can reduce conservatism in the design and hence yield a better solution. To demonstrate the advantage of using $\hat{y}$ as performance measures, the following ε_i are redefined, for example, by

$$\left.\begin{array}{lllll} \phi_1(p) & \triangleq & \Delta\hat{y}_1 & \leq & 45^\circ \\ \phi_2(p) & \triangleq & \Delta\hat{y}_2 & \leq & 0.025 \text{ pu} \\ \phi_3(p) & \triangleq & \Delta\hat{y}_3 & \leq & 0.002 \text{ pu} \\ \phi_4(p) & \triangleq & \Delta\hat{y}_4 & \leq & 0.20 \text{ pu} \end{array}\right\} . \tag{3.23}$$

By using the MBP algorithm, an acceptable design

$$p = \begin{bmatrix} 34.50 & 0.050 & 0.140 & 0.010 & 0.014 & 0.800 \end{bmatrix}^T ,$$

is found and the corresponding performance measures are

$$\begin{array}{lllll} \phi_1 & = & 44.95^\circ & (\leq & 45^\circ), \\ \phi_2 & = & 0.0242 \text{ pu} & (\leq & 0.025 \text{ pu}), \\ \phi_3 & = & 0.0015 \text{ pu} & (\leq & 0.002 \text{ pu}), \\ \phi_4 & = & 0.0151 \text{ pu} & (\leq & 0.20 \text{ pu}). \end{array}$$

The system's output responses to the test inputs are shown in Figure 3.9.

Table 3.2: Comparison of system's performances obtained by using $\hat{y}_i$ and $\tilde{y}_i$

i	$\Delta\hat{y}_i$	$\Delta\tilde{y}_i$
1	$43.27°$	$\leq$ $53.97°$
2	0.0263 pu	$\leq$ 0.0272 pu
3	0.0012 pu	$\leq$ 0.0012 pu
4	0.0154 pu	$\leq$ 0.0154 pu

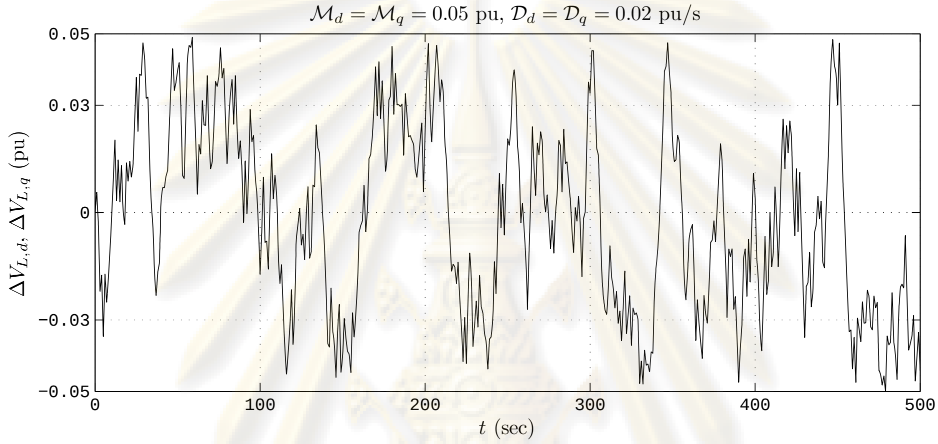

Figure 3.7: Test input waveform

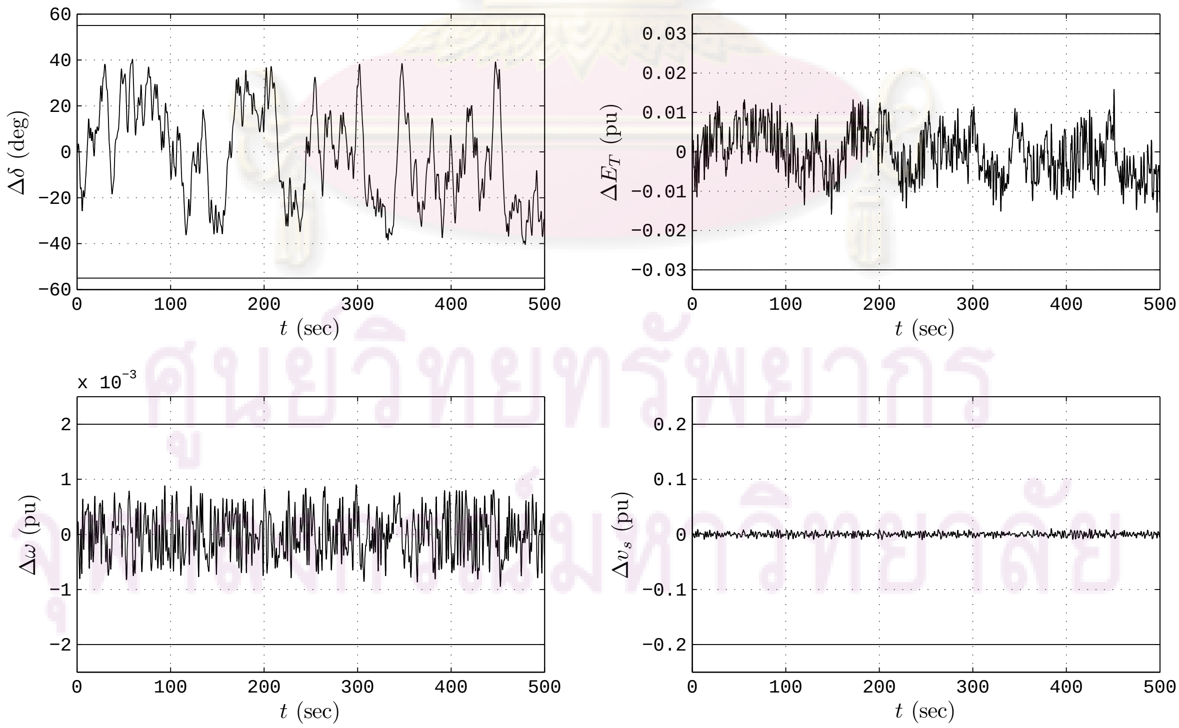

Figure 3.8: Output responses due to the test input (by using upper bounds as performance measures)

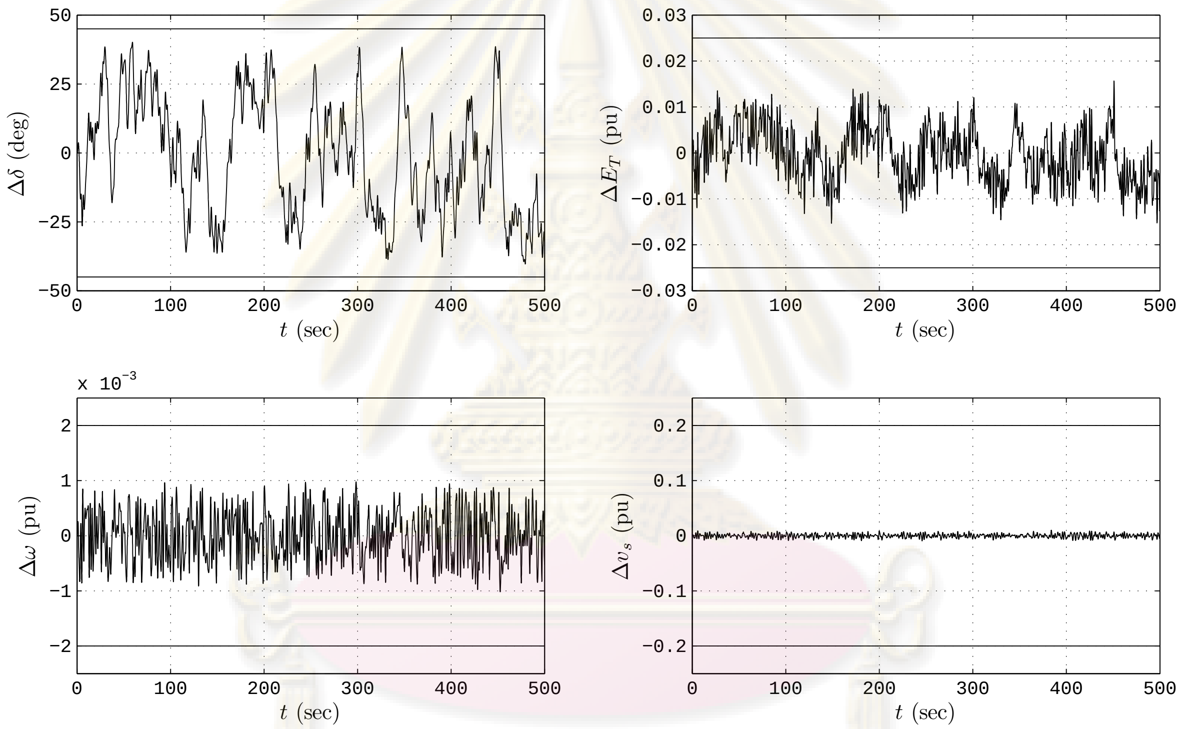

Figure 3.9: Output responses due to the test input (by using peak outputs as performance measures)

CHAPTER IV

ENHANCEMENT OF POWER SYSTEM'S STABILITY AND PERFORMANCES BY USING SVC

This chapter presents the improvement of stability and performances of power system subject to load voltage fluctuation by using SVC installed at the nearby bus.

4.1 Power System Model

The power system considered in this study is modelled as a single generator connecting to an infinite bus with an SVC installed at bus 2. The single line diagram of the system is shown in Fig. 4.1, where i_T denotes the generator current, e_T the terminal voltage of the generator, e_B the voltage at the infinite bus, v_2 the voltage at bus 2, v_L the load voltage at bus 4, L_{tr1} an inductance of a transformer connecting the generator to bus 2, L_{tr2} an inductance of a transformer connecting the bus 2 to bus 4 and L_l an inductance of the transmission line connecting bus 2 to the infinite bus.

By assuming that the power system operates under three-phase balanced condition, it follows that

$$\left.\begin{array}{lcl} e_T(t) & = & E_T(t)\sin(\omega t+\varphi_1) \\ v_2(t) & = & V_2(t)\sin(\omega t+\varphi_2) \\ v_L(t) & = & V_L(t)\sin(\omega t+\varphi_3) \\ i_T(t) & = & I_T(t)\sin(\omega t+\varphi_4) \end{array}\right\}, \qquad (4.1)$$

where φ_i $(i = 1, \ldots, 4)$ are the phase angles of e_T, v_2, v_L and i_T at the steady state.

Let ($E_{T,d}$, $V_{2,d}$, $V_{L,d}$, $I_{T,d}$) and ($E_{T,q}$, $V_{2,q}$, $V_{L,q}$, $I_{T,q}$) denote the d- and q-components of (E_T, V_2, V_L, I_T), respectively. One can readily show that the variables in the abc reference frame is related

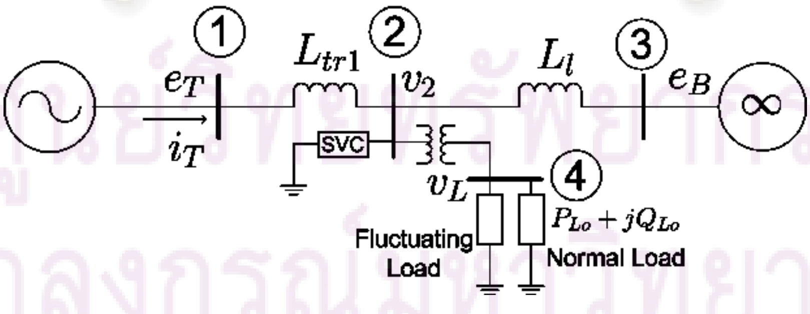

Figure 4.1: Power system configuration with an SVC installed at bus 2

to the dqo reference frame by

$$\left.\begin{array}{rcl} E_T(t) & = & \sqrt{E_{T,d}^2(t) + E_{T,q}^2(t)} \\ V_2(t) & = & \sqrt{V_{2,d}^2(t) + V_{2,q}^2(t)} \\ V_L(t) & = & \sqrt{V_{L,d}^2(t) + V_{L,q}^2(t)} \\ I_T(t) & = & \sqrt{I_{T,d}^2(t) + I_{T,q}^2(t)} \end{array}\right\}. \tag{4.2}$$

The power system considered here consists of a generator, an excitation system, a governor control loop and SVC. In the following subsections, models of each component are developed and then grouped as an interconnected system.

4.1.1 The Synchronous Generator Model

The generator is modelled as the following nonlinear differential equations [4]

$$\left.\begin{array}{rcl} \frac{dE_q'}{dt} & = & \frac{1}{T_{do}'}(-E_q' + (X_d - X_d')I_{T,d} + E_{\text{fd}}) \\ \frac{dE_d'}{dt} & = & \frac{1}{T_{qo}'}(-E_d' + (X_q - X_q')I_{T,q}) \\ \frac{d\delta}{dt} & = & \omega_b(\omega - \omega_s) = \omega_b \Delta\omega \\ \frac{d\Delta\omega}{dt} & = & \frac{1}{2H}(T_m - T_e - K_D\Delta\omega) \\ T_e & = & E_d' I_{T,d} + E_q' I_{T,q} + (X_q' - X_d')I_{T,d}I_{T,q} \end{array}\right\}, \tag{4.3}$$

where E_d' and E_q' are the transient electromotive forces, T_{do}' and T_{qo}' are the open circuit field time constants, X_d and X_q are the reactances, X_d' and X_q' are the transient reactances, E_{fd} is the field voltage, δ is the rotor angle of the generator, ω is the angular speed of the generator, H is the inertia constant, T_m is the mechanical input torque, T_e is the electrical input torque and K_D is the damping coefficient of the generator.

4.1.2 The Excitation System Model

The excitation system comprises a voltage transducer, an automatic voltage regulator (AVR) and a power system stabilizer (PSS). The block diagram of the excitation system is given in Fig. 4.2 and its state-space representation is

$$\left.\begin{array}{rcl} \frac{dm_1}{dt} & = & \frac{1}{T_R}(E_T - m_1) \\ \frac{dm_2}{dt} & = & K_s \frac{d\Delta\omega}{dt} - \frac{1}{T_W} m_2 \\ \frac{dm_3}{dt} & = & \frac{1}{T_2}(T_1 \frac{dm_2}{dt} + m_2 - m_3) \\ \frac{dm_4}{dt} & = & \frac{1}{T_4}(T_3 \frac{dm_3}{dt} + m_3 - m_4) \\ E_{\text{fd}} & = & K_A(V_{\text{ref}} - m_1 - v_s). \end{array}\right\}, \tag{4.4}$$

where m_i $(i = 1, \ldots, 4)$ denote the state variables, T_1, T_2 the lead-lag time constants of the excitation system, T_R is the transducer time constant, T_W is the washout time constant, K_s is the PSS gain, and

v_s is the output signal of the PSS described by

$$v_s = \begin{cases} v_s^{\min}, & m_4 < v_s^{\min}, \\ m_4, & v_s^{\min} \le m_4 \le v_s^{\max}, \\ v_s^{\max}, & m_4 > v_s^{\max}, \end{cases} \quad (4.5)$$

where $v_s^{\min}$ and $v_s^{\max}$ are some constants.

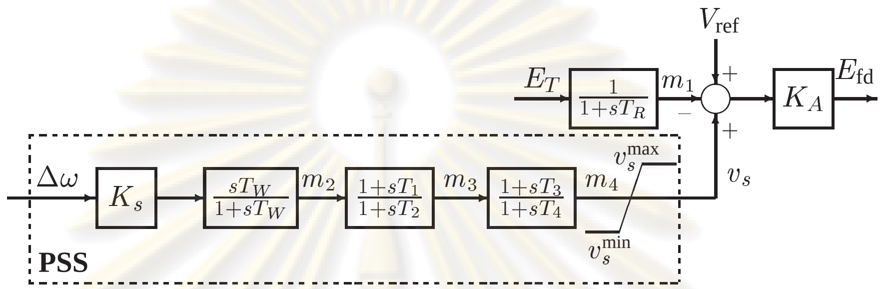

Figure 4.2: Block diagram of excitation system of power system with SVC installed at bus 2

4.1.3 The Governor Control Model

Fig. 4.3 shows the block diagram of the governor control loop. The differential equations describing this subsystem are given by

$$\left.\begin{aligned} \frac{dg_1}{dt} &= \frac{1}{T_G}\left(\frac{\Delta\omega}{R} - g_1\right) \\ \frac{dg_2}{dt} &= \frac{1}{T_P}(g_1 - g_2) \\ T_m &= T_{\text{ref}} - g_2 \end{aligned}\right\}, \quad (4.6)$$

where g_i $(i = 1, 2)$ are the state variables, K_I is the integrator gain, R is the droop constant, T_G is the governor time constant, and T_P is the prime mover time constant.

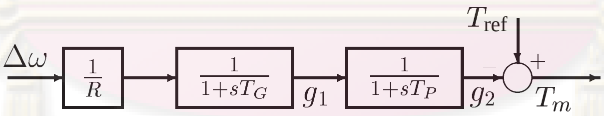

Figure 4.3: Block diagram of governor loop of power system with SVC installed at bus 2

4.1.4 The SVC Model

In this study, the SVC model as shown in Fig. 4.4 is taken from [23]. The model of the SVC is given by

$$\left.\begin{aligned} \frac{ds_1}{dt} &= \frac{1}{T_v}(K_v(V_{2o} - V_2) - s_1) \\ \frac{ds_2}{dt} &= \frac{1}{T_{v2}}\left(T_{v1}\frac{ds_1}{dt} + s_1 - s_2\right) \\ \frac{dB}{dt} &= \frac{1}{T_b}(B_{\text{ref}} - B) \end{aligned}\right\}, \quad (4.7)$$

where V_{2o} is the voltage of bus 2 at the steady state, K_v is the SVC gain, T_v is the SVC time constant, s_i $(i = 1, 2)$ are the state variables, (T_{v1}, T_{v2}) are the lead-lag time constants, T_b is the thyristor firing time constant, B is the susceptance of the SVC and B_{ref} is the output susceptance of the voltage regulator given by

$$B_{\text{ref}} = \begin{cases} B_{\min}, & s_2 < B_{\min}, \\ s_2, & B_{\min} \le s_2 \le B_{\max}, \\ B_{\max}, & s_2 > B_{\max}. \end{cases} \tag{4.8}$$

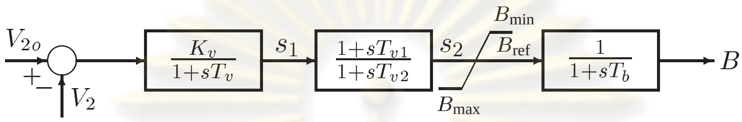

Figure 4.4: Block diagram of SVC

It is worth noting that, in order to ensure that the PSS and SVC models always operate in the linear ranges, the control signals m_4 and s_2 need to satisfy

$$\left.\begin{array}{ccccc} v_s^{\min} & \le & m_4 & \le & v_s^{\max} \\ B_{\min} & \le & s_2 & \le & B_{\max} \end{array}\right\}, \tag{4.9}$$

where $v_s^{\min}$, $v_s^{\max}$, $B_{\min}$ and $B_{\max}$ are some constants.

4.1.5 The Overall System Model

Owing to the very fast transient responses of the transmission network [4, 23], it is sufficient to represent the transmission network with the algebraic equation

$$I(x, V) = Y_N V, \tag{4.10}$$

where x is the state vector, V is the bus voltage vector and I is the current injection vector.

Accordingly, the overall system equations, including the differential equations for all the devices and the algebraic equations for the transmission network (4.10), are expressed as

$$\frac{dx}{dt} = w(x, V), \tag{4.11}$$

where w is a vector of corresponding nonlinear function.

Define the output vector of interest y, the input vector u and the state vector x as follows:

$$\left.\begin{array}{lcl} y & \triangleq & [\delta \quad E_T \quad V_2 \quad m_4 \quad s_2]^T \\ u & \triangleq & V_L\angle\theta \\ x & \triangleq & [\ \delta \quad \Delta\omega \quad E'_q \quad E'_d \quad m_1 \quad m_2 \quad m_3 \quad m_4 \quad g_1 \quad g_2 \quad s_1 \quad s_2 \quad s_3\ ]^T \end{array}\right\}, \tag{4.12}$$

where $V_L\angle\theta$ is the phasor of the voltage of bus 2.

The generator parameters (in per unit with respect to 2220 MVA base) are shown in Tab. 4.1, and the power system is in the steady state with the following conditions:

$$P_o = 0.9 \text{ pu}, \quad Q_o = 0.436 \text{ pu}, \quad E_{To} = 1.0 \text{ pu}, \quad E_{Bo} = 0.9 \text{ pu} \quad V_{Lo} = 0.732 \text{ pu}.$$

By applying the steady-state analysis given in [4], one obtains a nominal operating point

$$x_o = \left[\ \delta_o \quad \Delta\omega_o \quad E'_{qo} \quad E'_{do} \quad m_{1o} \quad m_{2o} \quad m_{3o} \quad m_{4o} \quad g_{1o} \quad g_{2o} \quad s_{1o} \quad s_{2o} \quad s_{3o}\ \right]^T, \qquad (4.13)$$

where $\delta_o = 46.26°$, $E'_{qo} = 0.3170$ pu, $E'_{do} = 1.0875$ pu and all others are zero.

Equation (4.11) is linearized about the nominal operating point in (4.13) and the incremental linear model is given by

$$\left.\begin{array}{rcl} \frac{d\Delta x}{dt} & = & A\Delta x + B\Delta u \\ \Delta y & = & C\Delta x + D\Delta u \end{array}\right\}, \qquad (4.14)$$

where A, B, C and D are constant matrices, and Δu, Δx, and Δy are the incremental input, state, and output vectors, respectively.

4.2 Characterization of the Possible Set

This section describes how to characterize the possible set $\mathcal{P}$. Assume that the power system is in the steady state for $t \leq 0$ and the load voltage changes for $t > 0$. That is,

$$v_L(t) = \left\{ \begin{array}{cc} V_{Lo}\sin(\omega t + \theta), & t \leq 0 \\ (V_{Lo} + \Delta V_L(t))\sin(\omega t + \theta), & t > 0 \end{array} \right\}, \qquad (4.15)$$

where V_{Lo} is constant and depends upon the nominal operating condition of the system. Accordingly, the set $\mathcal{P}$ is defined as

$$\mathcal{P} \triangleq \left\{ \Delta V_L : \Delta V_L(0) = 0, \|\Delta V_L\|_\infty \leq \mathcal{M}, \|\Delta \dot{V}_L\|_\infty \leq \mathcal{D} \right\}, \qquad (4.16)$$

where $\mathcal{M}$ and $\mathcal{D}$ are some positive numbers.

4.3 Design Formulation

In the following design, assume that the load voltage variation ΔV_L applies to the power system for $t > 0$. The SVC will be used for improving the performance of the power system where the signal ΔV_2 is fedback to the SVC. The configuration of the feedback control system is shown in Fig. 4.5.

To ensure good performances for the power system, it is required that, for any disturbance $\Delta V_L \in \mathcal{P}$ and for all time $t > 0$,

Table 4.1: Generator parameters in per unit base

K_D	=	10	H	=	3.5 sec	K_A	=	100
K_s	=	19.03	L_{tr}	=	0.15 pu	L_{l_1}	=	0.5 pu
L_{l_2}	=	0.93 pu	T'_{do}	=	8.0 sec	T'_{qo}	=	1.0 sec
T_G	=	0.2 sec	T_P	=	0.3 sec	T_R	=	0.015 sec
T_W	=	0.844 sec	T_1	=	0.137 sec	T_2	=	0.058 sec
T_3	=	0.225 sec	T_4	=	0.158 sec	R	=	0.05
X_d	=	1.81 pu	X_q	=	1.76 pu	R_s	=	0.003 pu
X'_d	=	0.30 pu	X'_q	=	0.65 pu			

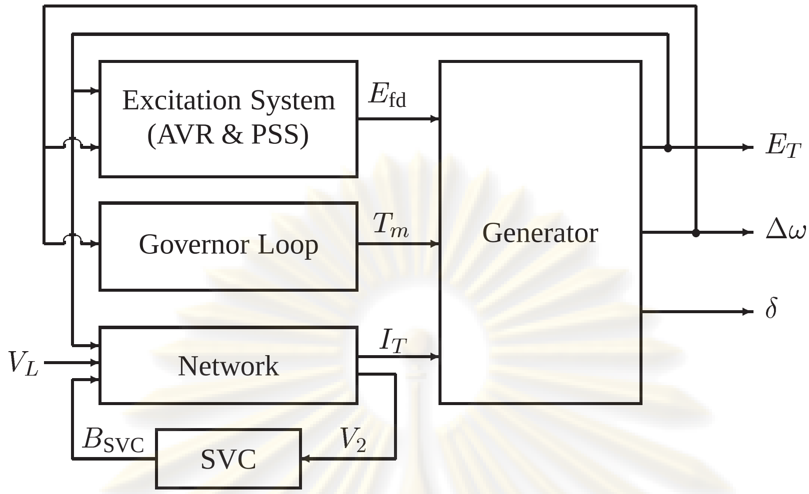

Figure 4.5: Configuration of the power system with SVC installed at bus 2

- the incremental rotor angle, the incremental terminal voltage of the generator and the incremental voltage of the nearby bus remain strictly within the prescribed bounds;
- the signals m_4 and s_2 remain within their linear ranges of operation.

Let p and q denote the design parameter vectors of the PSS and the SVC, respectively. That is to say,

$$p \triangleq \begin{bmatrix} K_s & T_w & T_1 & T_2 & T_3 & T_4 \end{bmatrix}^T, \quad q \triangleq \begin{bmatrix} K_v & T_v & T_{v1} & T_{v2} \end{bmatrix}^T.$$

From the above requirements, the principal design specifications are expressed as

$$\left.\begin{array}{rcccl} \phi_1(p) & \triangleq & \Delta\tilde{y}_1 & \leq & \varepsilon_1 \\ \phi_2(p) & \triangleq & \Delta\tilde{y}_2 & \leq & \varepsilon_2 \\ \phi_3(p) & \triangleq & \Delta\tilde{y}_3 & \leq & \varepsilon_3 \\ \phi_4(p) & \triangleq & \tilde{y}_4 & \leq & \varepsilon_4 \\ \phi_5(p) & \triangleq & \tilde{y}_5 & \leq & \varepsilon_5 \end{array}\right\}, \tag{4.17}$$

where ε_i $(i = 1, \ldots, 5)$ are the largest values of ϕ_i that are acceptable. In this work, the following bounds ε_i (which is based on a practical operating criteria [4]) are used:

$$\varepsilon_1 = 20^\circ, \quad \varepsilon_2 = 0.03 \text{ pu}, \quad \varepsilon_3 = 0.05 \text{ pu}, \quad \varepsilon_4 = 0.2 \text{ pu}, \quad \varepsilon_5 = 1 \text{ pu}. \tag{4.18}$$

Notice that (4.17) shows the multiobjective nature of the design problem.

4.4 Numerical Results

At this point, the possible set $\mathcal{P}$ needs to be defined. Accordingly, the bound $\mathcal{M}$ is chosen with respect to the change of real power of the load bus that used to happen or is likely to happen in practice. The bound $\mathcal{D}$ is related to the rate of change of the power flow from the transmission network to the fluctuating load. In this study, the bounds used are chosen, for example, by $\mathcal{M} = 0.2$ pu and $\mathcal{D} = 0.2$ pu/s.

To shed some light on the physical meaning of only the condition $\mathcal{M} = 0.2$ pu, suppose that the system was in sinusoidal steady-state. Recall that the power base of the generator is 2220 MW. By performing load-flow calculation, it is found that if the load voltage decreased (or increased) 0.2 pu from its nominal value, then the real power would be drawn from (or injected into) the load bus by 275.66 MW (or 210.90 MW). This would give a rough idea of the change of the power flow in the system. However, for more accurate information of the change of the power flow in connection with $\mathcal{M} = 0.2$ pu and $\mathcal{D} = 0.2$ pu/s, more work needs to be done and this would be a topic worth of further investigation.

4.4.1 Design of SVC by Using the Upper Bounds of the Peak Outputs

In this subsection, we make use of the upper bounds of the peak outputs $\tilde{y}$ as performance measures.

Consider the power system without the SVC. The system has only the PSS in the excitation system. In this regard, the PSS is to be tuned first so as to satisfy the specifications ϕ_i $(i = 1, \ldots 4)$ of (4.17). After a number of trials, it appears that the MBP algorithm cannot locate a vector p such that the requirements ϕ_i $(i = 1, \ldots 4)$ of (4.17) are satisfied. By performing a number of iterations, the following p is obtained

$$p = \begin{bmatrix} 34.50 & 0.023 & 0.230 & 0.010 & 0.014 & 0.950 \end{bmatrix},$$

and the corresponding performances of the system with respect to the requirements (4.18) are given by

$$\left.\begin{array}{lcll} \phi_1 & = & 14.62^\circ & (\leq \;\; 20^\circ) \\ \phi_2 & = & 0.023 \text{ pu} & (\leq \;\; 0.03 \text{ pu}) \\ \phi_3 & = & 0.092 \text{ pu} & (> \;\; 0.05 \text{ pu}) \\ \phi_4 & = & 0.015 \text{ pu} & (\leq \;\; 0.2 \text{ pu}) \end{array}\right\}. \tag{4.19}$$

It can be seen from (4.19) that only ϕ_3 does not satisfy the requirement. In this case, it clearly shows that the power system without the SVC cannot be used to limit the voltage fluctuation of the nearby bus.

Accordingly, in order to provide sufficient damping in compensation for load voltage fluctuation, the SVC (see (4.7)) is installed at the nearby bus and is then taken into a design process. By starting from $q = [0,\, 0,\, 0,\, 0]^T$ and after a number of iterations, the MBP algorithm locates a design solution of inequalities (4.17).

$$q = \begin{bmatrix} 28.0 & 0.150 & 0.169 & 0.033 \end{bmatrix}^T, \tag{4.20}$$

and the corresponding performance measures are

$$\left.\begin{array}{lcll} \phi_1 & = & 5.16^\circ & (\leq \;\; 20^\circ) \\ \phi_2 & = & 0.008 \text{ pu} & (\leq \;\; 0.03 \text{ pu}) \\ \phi_3 & = & 0.034 \text{ pu} & (\leq \;\; 0.05 \text{ pu}) \\ \phi_4 & = & 0.004 \text{ pu} & (\leq \;\; 0.2 \text{ pu}) \\ \phi_5 & = & 0.94 \text{ pu} & (\leq \;\; 1 \text{ pu}) \end{array}\right\}. \tag{4.21}$$

To verify the design results, a random test input is generated as a piecewise linear function such that its magnitude and its slope are bounded by 0.2 pu and 0.2 pu/s, respectively. The waveform of a random test input is shown in Fig. 4.6. The system's responses to the test input for the system without and with the SVC are shown in Figs. 4.7 and 4.8, respectively.

By using the linearized model based on small signal assumption, it is suggested that the disturbance impinging on the system be less than or equal 1% from its nominal value. Although the voltage deviation of 0.2 pu from its nominal value is considered as a large disturbance (with respect to the 2220 MW base of the generator), the simulation results so obtained agree well with those obtained from the actual nonlinear systems. Hence, the linearized model used in this work is still valid.

Clearly, the system with the SVC provides a better damping to the system so that all outputs of interest satisfy the design specification.

4.4.2 Design of SVC by Using the Peak Outputs

In this subsection, we use of the peak outputs $\hat{y}_i$ defined in chapter 2 as performance measures. By using the MBP algorithm, the satisfactory design parameters are the same as those obtained in the previous subsection and the corresponding performance measures are

$$\left.\begin{array}{lcll} \phi_1 & = & 3.48^\circ & (\leq \;\; 20^\circ) \\ \phi_2 & = & 0.007 \text{ pu} & (\leq \;\; 0.03 \text{ pu}) \\ \phi_3 & = & 0.033 \text{ pu} & (\leq \;\; 0.05 \text{ pu}) \\ \phi_4 & = & 0.004 \text{ pu} & (\leq \;\; 0.2 \text{ pu}) \\ \phi_5 & = & 0.92 \text{ pu} & (\leq \;\; 1 \text{ pu}) \end{array}\right\} . \tag{4.22}$$

Table 4.2 shows the peak outputs of the system with the SVC parameters obtained in the design by using the upper bounds of peak outputs as performance measures. Note that the value of peak outputs are less than or equal to thier upper bounds.

Table 4.2: Comparison of performances of power system with SVC obtained by using $\hat{y}_i$ and $\tilde{y}_i$

i	$\Delta\hat{y}_i$	$\Delta\tilde{y}_i$
1	3.48°	$\leq\ 5.16^\circ$
2	0.007 pu	$\leq\ 0.008$ pu
3	0.033 pu	$\leq\ 0.034$ pu
4	0.004 pu	$\leq\ 0.004$ pu
5	0.92 pu	$\leq\ 0.94$ pu

Accordingly, using the peak outputs $\hat{y}_i$ as performance measures can reduce conservatism in the design and hence yield a better solution.

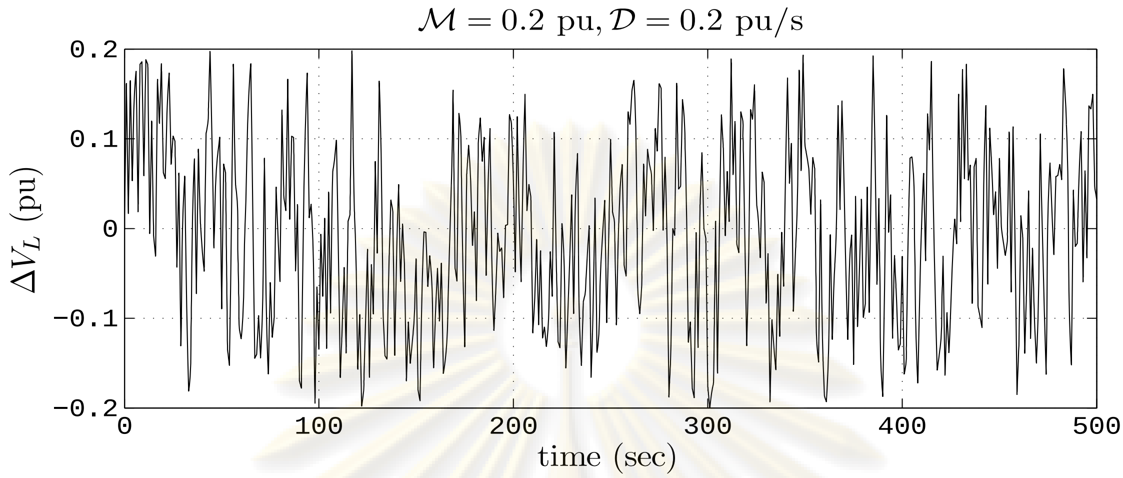

Figure 4.6: Test input waveform

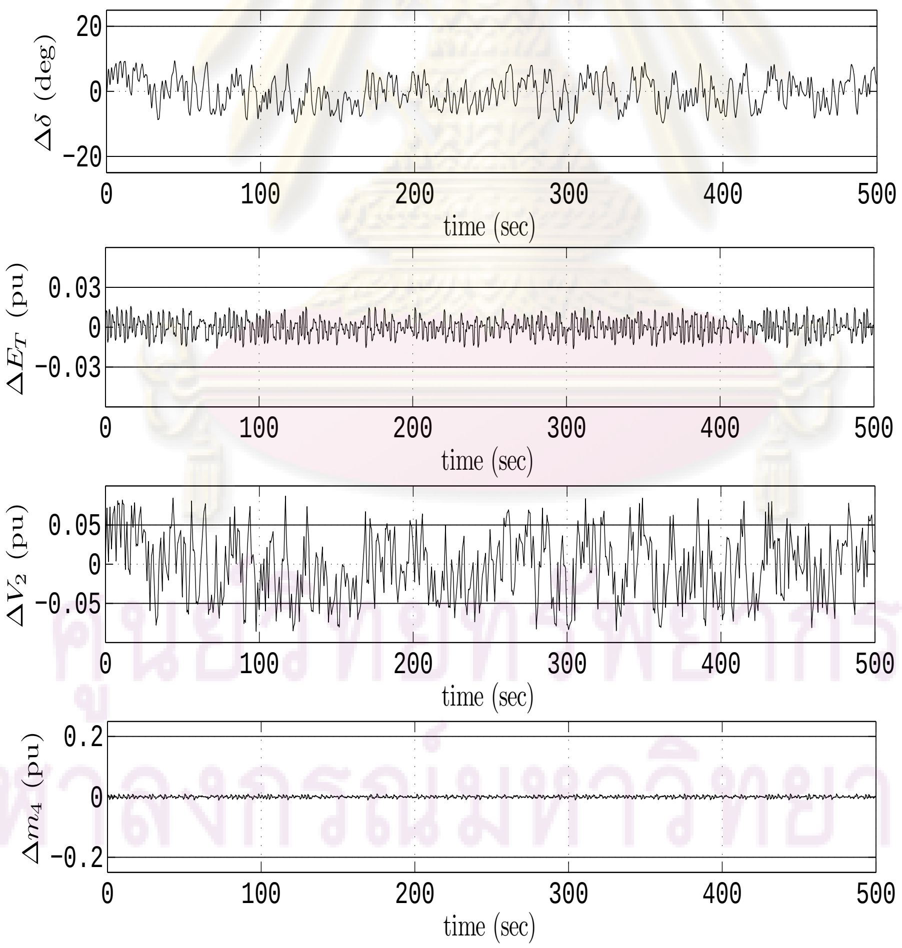

Figure 4.7: Responses of the power system without SVC due to the test input

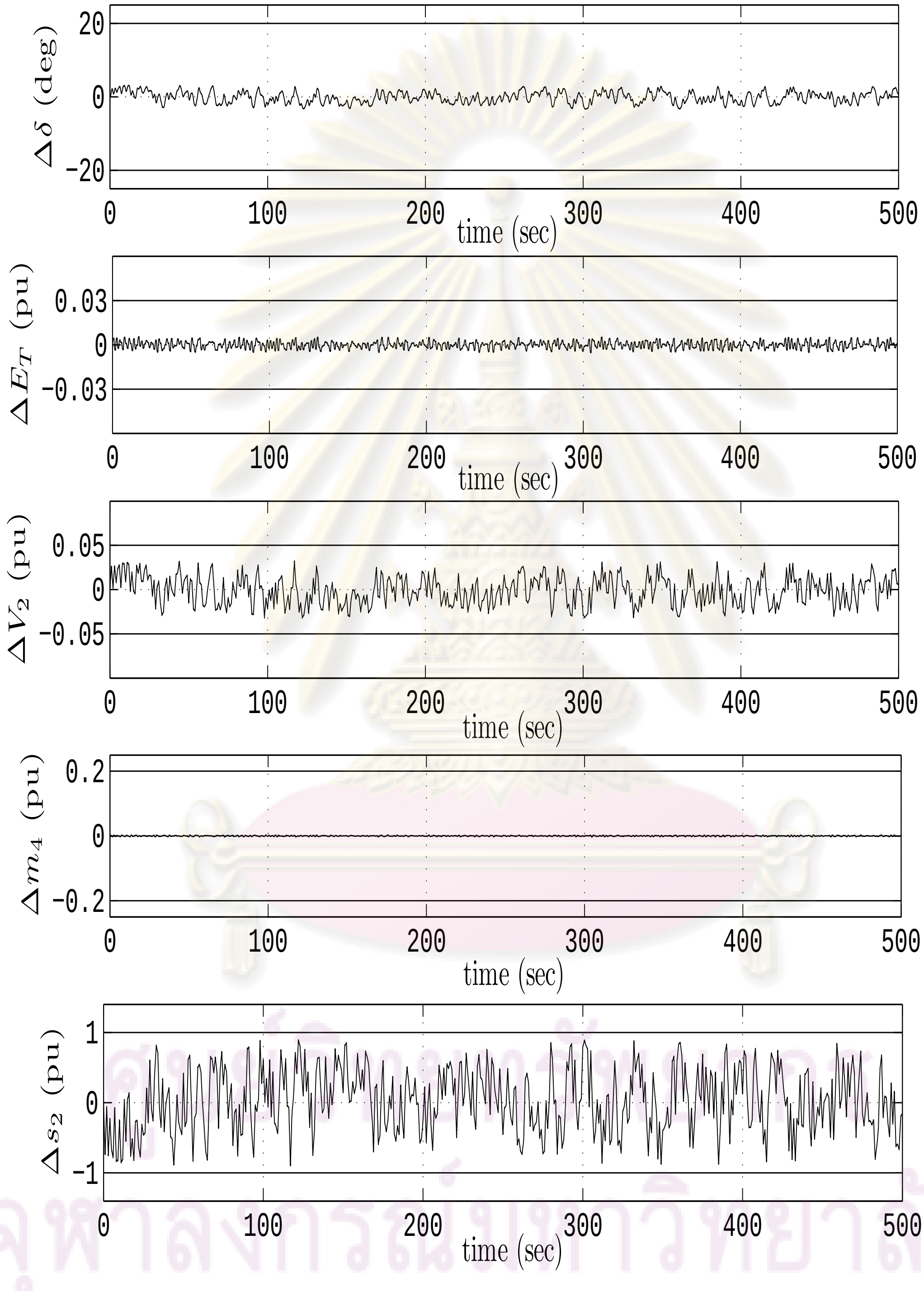

Figure 4.8: Responses of the power system with SVC due to the test input

CHAPTER V

CONCLUSIONS

5.1 Summary

This thesis describes a general procedure for designing a device such as PSS and SVC for power systems subject to load voltage variations by Zakian's framework, comprising the principle of matching and the method of inequalities. The framework is effective and facilitates a realistic formulation of the design problem. The numerical results clearly show that all the outputs y of interest can be ensured to remain strictly within the prescribed bounds. Moreover, by virtue of the framework, the stability and the satisfactory performances of the power system can be ensured as long as the load voltage variation satisfies (2.3).

To improve the system's performances in the generating unit (e.g., the rotor angle, the terminal voltage and the speed deviation of the generator), only PSS in the excitation system can effectively compensate those performances of power systems. Once the system's performance of interest is not in the generating unit, the performance may not be met the design specification by using only PSS. For instance, when the voltage of the nearby load bus is taken into consideration, only PSS fails to limit the voltage fluctuation due to the large load variation. It is necessary to make use of an SVC to provide sufficient damping to the system.

By using the convenient upper bounds of the peak outputs as the performance measures in the design process, MBP can sometimes fail to find the solution of the set of design inequalities. This may be due to the conservatism in using the upper bounds as the performance measures. Accordingly, it is suggested that the exact peak outputs be used instead of their upper bounds so as to avoid the conservatism due to the performance measures used.

5.2 Further Improvements

This section introduces some further improvements that will help enhance the virtue of this research work.

1. Because of the potential in the framework, it will be fruitful to develop a practical method for determining $\mathcal{M}$ and $\mathcal{D}$, for example, for applications in which an electric arc furnace is in operation and causes voltage fluctuation. By assuming that the power system was in the sinusoidal steady-state, one can perform the power-flow criterion to determine the bounds $\mathcal{M}$ and $\mathcal{D}$, given the physical data of the consumed (or injected) real power at the load bus.

2. In this thesis, the proposed method of designing compensators deals with the power system having a single operating point. However, in practical power systems, the operating point may

change from one to another according to the conditions which the power system is subjected to. Hence, when the operating condition of power systems changes, a new design with respect to the new operating condition can be obtained systematically by using the framework adopted in this work.

3. In Chapter 3, the power system's model includes the dynamic behavior of the transmission network. Although the transmission network has very fast transient responses and can be neglected, the methodology of computing the performance measures used in this thesis is still valid to the full model (which considers the dynamic effect of the network) as well as large interconnected power systems in practice.

5.3 Possible Extensions

1. The PSS and the SVC are used in this thesis for improving stability and dynamic performances of power systems. However, the framework adopted here is also applicable to other types of compensator.

2. In practice, the power system consists of a number of generators, which is called the multi-machine system. The Zakian's framework can deal with the multi-machine system as well.

REFERENCES

[1] C. J. Wu, S. S. Shong, W. N. Chang, C. N. Cheng, C. H. Li and T. Y. Guo (1999). Enhancement of static excitation system performance for generators near electric arc furnace loads, *IEEE Transactions on Energy Conversion* 14: 225–231.

[2] C. J. Wu, Y. S. Chuang, C. P. Huang and Y. P. Chang (2007). Tuning of static excitation systems to improve dynamic performance for generators serving electric arc furnaces loads, *IEEE Transactions on Energy Conversion* 22: 350–357.

[3] C. S. Chen, H. J. Chuang, C. T. Hsu and S. M. Tseng (2001). Mitigation of voltage fluctuation for an industrial customer with arc furnace, *Proceedings of Power Engineering Society Summer Meeting*: 1610–1615.

[4] P. Kunder (1994). *Power System Stability and Control*, McGraw-Hill, New York.

[5] P. S. Sensarma, K. R. Padiyar and V. Ramanarayanan (2001). Analysis and performance evaluation of a distribution STATCOM for compensating voltage fluctuations, *IEEE Transactions on Power Delivery* 16: 259–264.

[6] Q. Zhao and J. Jiang (1995). Robust SVC controller design for improving power system damping, *IEEE Transactions on Power Systems* 10: 1927–1932.

[7] H. C. Tay and M. F. Conlon (1998). Development of a SMES system as a fluctuating load compensator, *Proceedings of the IEE* 6: 700–706.

[8] O. Sakamoto, M. Hashimoto, M. Sonoda and T. Nitta (2005). Effects of superconducting generator on mitigation of voltage fluctuation in power systems with wind power generation, *15th Power Systems Computation Conference*: 1–6.

[9] P. G. Lane (1992). *Design of Control Systems with Inputs and Outputs Satisfying Certain Bounding Conditions*, PhD thesis, UMIST, Manchester, UK.

[10] V. Zakian and U. Al-Naib (1973). Design of dynamical and control systems by the method of inequalities, *Proceedings of the IEE* 120: 1421–1427.

[11] V. Zakian (1975). Proproties of I_{MN} and J_{MN} approximants and applications to numercial inversion of Laplace transforms and initial value problems, *Journal of Mathematical Analysis and Applications* 50: 191–222.

[12] V. Zakian (1979). New formulation for the method of inequalities, *Proceedings of the IEE* 126: 579–584.

[13] V. Zakian (1987). Design formulations, *International Journal of Control* 46: 403–408.

[14] V. Zakian (1996). Perspectives of the principle of matching and the method of inequalities, *International Journal of Control* 65: 147–175.

[15] V. Zakian, editor (2005). *Control Systems Design: A New Framework*, Springer-Verlag, London.

[16] W. Silpsrikul and S. Arunsawatwong (2009). Computation of peak output for inputs restricted in L_2 and L_∞ norms using finite difference schemes and convex optimization, *International Journal of Automation and Computing* 6: 10–16.

[17] J. S. Sturm (1999). Use SeDuMi 1.02, a Matlab toolbox for optimization over symmetric cones. *Optimization Methods and Software* 11&12: 625–653.

[18] A. R. Mahran, B. W. Hogg and M. L. El-Sayed (1992). Co-ordinated control of synchronous generator excitation and static var compensator, *IEEE Transactions on Energy Conversion* 7: 615–622.

[19] R. You and M. H. Nehrir (2004). A systemmatic approach to controller design for SVC to enhance damping of power system oscillations, *Power System Conference and Exposition* 2: 1134–1139.

[20] S. Arabi, G. J. Rogers, D. Y. Wong, P. Kunder and M. G. Laudy (1991). Small signal stability program analysis of SVC and HVDC in AC power system, *IEEE Transactions on Power Systems* 6: 1147–1153.

[21] J. F. Whidborne (1993). EMS control system design for a maglev vehicle – A critical system, *Automatica* 29: 1345–1349.

[22] S. Arunsawatwong (2005). Critical control of building under seismic disturbance, Chapter 13 in *V. Zakian (editor), Control Systems Design: A New Framework*, Springer-Verlag, London.

[23] IEEE Special Stability Controls Working Groups (1994). Static var compensator models for power flow and dynamic performance simulation, *IEEE Transactions on Power Systems* 9: 229–240.

APPENDICES

APPENDIX A

Park's Transformation

Let f denote a network variable (current or voltage) of interest and subscripts (a, b, c) be the components of f in the phases (a, b, c). The transformation of (f_a, f_b, f_c) into (F_d, F_q, F_o) is call Park's transformation and is given by

$$F_{dqo} \triangleq K(\theta) f_{abc}, \tag{1}$$

where $\theta = \omega t$ denotes the rotor angle position of the generator, the vector f_{abc} and F_{abc} is defined as

$$f_{abc} \triangleq \begin{bmatrix} f_a & f_b & f_c \end{bmatrix}^T, \quad F_{dqo} \triangleq \begin{bmatrix} F_d & F_q & F_o \end{bmatrix}^T, \tag{2}$$

and $K(\theta)$ is given by

$$K(\theta) \triangleq \frac{2}{3} \begin{bmatrix} \cos\theta & \cos(\theta - \frac{2\pi}{3}) & \cos(\theta + \frac{2\pi}{3}) \\ -\sin\theta & -\sin(\theta - \frac{2\pi}{3}) & -\sin(\theta + \frac{2\pi}{3}) \\ \frac{1}{2} & \frac{1}{2} & \frac{1}{2} \end{bmatrix}. \tag{3}$$

It is important to note that the three-phase system under the assumption of balanced condition yields the following statements.

- One can define (f_a, f_b, f_c) as

$$\left.\begin{array}{l} f_a(t) = F_a(t)\sin(\omega t + \varphi_a) \\ f_b(t) = F_b(t)\sin(\omega t + \varphi_b) \\ f_c(t) = F_c(t)\sin(\omega t + \varphi_c) \end{array}\right\}, \tag{4}$$

  where ω is the angular speed of the generator, and (φ_a, φ_b, φ_c) are the phase angles of (f_a, f_b, f_c) at the steady state.

- The components (F_a, F_b, F_c) are equal (i.e., $F_a = F_b = F_c$).

- There exist only components of the d- and q-variables and the o-component is zero, i.e., $F_o(t) = 0$.

- The component F_a can be written in terms of F_d and F_q as

$$F_a = \sqrt{F_d^2 + F_q^2}. \tag{5}$$

By applying the transformation (1) to the variables e_T, i_T and v_L (which are all in the abc reference frame under the condition that the three phase system is balanced) in (3.1), one can take the following steps to derive the transmission network model in the dqo reference frame. First, we write (3.1) in the matrix form

$$\begin{bmatrix} e_{T,a} \\ e_{T,b} \\ e_{T,c} \end{bmatrix} = \begin{bmatrix} L_{tr} & 0 & 0 \\ 0 & L_{tr} & 0 \\ 0 & 0 & L_{tr} \end{bmatrix} \frac{d}{dt} \begin{bmatrix} i_{T,a} \\ i_{T,b} \\ i_{T,c} \end{bmatrix} + \begin{bmatrix} v_{L,a} \\ v_{L,b} \\ v_{L,c} \end{bmatrix}. \tag{6}$$

After rewriting (6) in terms of the *dqo* variables, we have

$$\begin{aligned} K^{-1}\begin{bmatrix} E_{T,d} \\ E_{T,q} \\ E_{T,o} \end{bmatrix} &= \begin{bmatrix} L_{tr} & 0 & 0 \\ 0 & L_{tr} & 0 \\ 0 & 0 & L_{tr} \end{bmatrix} \frac{d}{dt}\left(K^{-1}\begin{bmatrix} I_{T,d} \\ I_{T,q} \\ I_{T,o} \end{bmatrix} \right) + K^{-1}\begin{bmatrix} V_{L,d} \\ V_{L,q} \\ V_{L,o} \end{bmatrix} \\ &= \begin{bmatrix} L_{tr} & 0 & 0 \\ 0 & L_{tr} & 0 \\ 0 & 0 & L_{tr} \end{bmatrix} \left(K^{-1}\frac{d}{dt}\begin{bmatrix} I_{T,d} \\ I_{T,q} \\ I_{T,o} \end{bmatrix} + \frac{dK^{-1}}{dt}\begin{bmatrix} I_{T,d} \\ I_{T,q} \\ I_{T,o} \end{bmatrix} \right) + K^{-1}\begin{bmatrix} V_{L,d} \\ V_{L,q} \\ V_{L,o} \end{bmatrix}. \end{aligned} \tag{7}$$

Multiplying K on both sides of (7) gives

$$\begin{bmatrix} E_{T,d} \\ E_{T,q} \\ E_{T,o} \end{bmatrix} = \begin{bmatrix} L_{tr} & 0 & 0 \\ 0 & L_{tr} & 0 \\ 0 & 0 & L_{tr} \end{bmatrix} \left(\frac{d}{dt}\begin{bmatrix} I_{T,d} \\ I_{T,q} \\ I_{T,o} \end{bmatrix} + K\frac{dK^{-1}}{dt}\begin{bmatrix} I_{T,d} \\ I_{T,q} \\ I_{T,o} \end{bmatrix} \right) + \begin{bmatrix} V_{L,d} \\ V_{L,q} \\ V_{L,o} \end{bmatrix}. \tag{8}$$

Substituting $K\frac{dK^{-1}}{dt}$ into (8) yields

$$\begin{bmatrix} E_{T,d} \\ E_{T,q} \\ E_{T,o} \end{bmatrix} = \begin{bmatrix} L_{tr} & 0 & 0 \\ 0 & L_{tr} & 0 \\ 0 & 0 & L_{tr} \end{bmatrix} \left(\frac{d}{dt}\begin{bmatrix} I_{T,d} \\ I_{T,q} \\ I_{T,o} \end{bmatrix} + \begin{bmatrix} -\omega I_{T,q} \\ \omega I_{T,d} \\ 0 \end{bmatrix} \right) + \begin{bmatrix} V_{L,d} \\ V_{L,q} \\ V_{L,o} \end{bmatrix}. \tag{9}$$

Hence, under the condition that the system is balanced, the o-component vanishes and the model of the transmission network is described by (3.3).

APPENDIX B

Corresponding Matrices of Power System Model described in the chapter 3

The constant matrices $T \in \mathbb{R}^{13\times 13}$ and $E \in \mathbb{R}^{13\times 4}$ of (3.10) developed in Section 3.1.5 are given by

$$T = \left[\begin{array}{ccccccccccccc}
0 & \omega_b & 0 & 0 & 0 & 0 & 0 & 0 & 0 & 0 & 0 & 0 & 0 \\
0 & -\frac{K_D}{2H} & 0 & 0 & 0 & 0 & 0 & 0 & 0 & 0 & 0 & 0 & -\frac{1}{2H} \\
0 & 0 & -\frac{1}{T'_{do}} & 0 & -\frac{X_d - X'_d}{T'_{do}} & 0 & -\frac{K_A}{T'_{do}} & 0 & 0 & \frac{K_A}{T'_{do}} & 0 & 0 & 0 \\
0 & 0 & 0 & -\frac{1}{T'_{qo}} & 0 & \frac{X_q - X'_q}{T'_{qo}} & 0 & 0 & 0 & 0 & 0 & 0 & 0 \\
0 & 0 & 0 & \frac{1}{L_{tr}} & -\frac{R_s}{L_{tr}} & \frac{X'_q}{L_{tr}} + \omega_s & 0 & 0 & 0 & 0 & 0 & 0 & 0 \\
0 & 0 & \frac{1}{L_{tr}} & 0 & -(\frac{X'_d}{L_{tr}} + \omega_s) & -\frac{R_s}{L_{tr}} & 0 & 0 & 0 & 0 & 0 & 0 & 0 \\
0 & 0 & 0 & 0 & 0 & 0 & -\frac{1}{T_R} & 0 & 0 & 0 & 0 & 0 & 0 \\
0 & -\frac{K_D K_s}{2H} & 0 & 0 & 0 & 0 & 0 & -\frac{1}{T_W} & 0 & 0 & 0 & 0 & -\frac{K_s}{2H} \\
0 & -\frac{K_D K_s T_1}{2HT_2} & 0 & 0 & 0 & 0 & 0 & \frac{1}{T_2}(1 - \frac{T_1}{T_W}) & -\frac{1}{T_2} & 0 & 0 & 0 & -\frac{K_s T_1}{2HT_2} \\
0 & -\frac{K_D K_s T_1 T_3}{2HT_2 T_4} & 0 & 0 & 0 & 0 & 0 & T_3 - \frac{T_1 T_3}{T_W} & \frac{1}{T_4} - T_3 & -\frac{1}{T_4} & 0 & 0 & -\frac{K_s T_1 T_3}{2HT_2 T_4} \\
0 & \frac{K_I}{R} & 0 & 0 & 0 & 0 & 0 & 0 & 0 & 0 & 0 & 0 & 0 \\
0 & \frac{1}{RT_G} & 0 & 0 & 0 & 0 & 0 & 0 & 0 & 0 & \frac{1}{T_G} & -\frac{1}{T_G} & 0 \\
0 & 0 & 0 & 0 & 0 & 0 & 0 & 0 & 0 & 0 & 0 & \frac{1}{T_P} & -\frac{1}{T_P}
\end{array}\right],$$

$$E = \left[\begin{array}{ccccccccccccc}
0 & 0 & \frac{K_A}{T'_{do}} & 0 & 0 & 0 & 0 & 0 & 0 & 0 & 0 & 0 & 0 \\
0 & \frac{1}{2H} & 0 & 0 & 0 & 0 & 0 & \frac{K_s}{2H} & \frac{K_s T_1}{2HT_2} & \frac{K_s T_1 T_3}{2HT_2 T_6} & 0 & 0 & 0 \\
0 & 0 & 0 & 0 & -\frac{1}{L_{tr}} & 0 & 0 & 0 & 0 & 0 & 0 & 0 & 0 \\
0 & 0 & 0 & 0 & 0 & -\frac{1}{L_{tr}} & 0 & 0 & 0 & 0 & 0 & 0 & 0
\end{array}\right]^T.$$

After linearizing (3.10) and (3.11) around a nominal point, the corresponding matrices A, B, C and D are expressed as follows:

$$
A = \begin{bmatrix}
0 & \omega_b & 0 & 0 & 0 & 0 & 0 & 0 & 0 & 0 & 0 & 0 & 0 \\
0 & -\frac{K_D}{2H} & a_{2,3} & a_{2,4} & a_{2,5} & a_{2,6} & 0 & 0 & 0 & 0 & 0 & 0 & -\frac{1}{2H} \\
0 & 0 & -\frac{1}{T'_{do}} & 0 & -\frac{X_d - X'_d}{T'_{do}} & 0 & -\frac{K_A}{T'_{do}} & 0 & 0 & \frac{K_A}{T'_{do}} & 0 & 0 & 0 \\
0 & 0 & 0 & -\frac{1}{T'_{qo}} & 0 & \frac{X_q - X'_q}{T'_{qo}} & 0 & 0 & 0 & 0 & 0 & 0 & 0 \\
0 & a_{5,2} & 0 & \frac{1}{L_{tr}} & -\frac{R_s}{L_{tr}} & a_{5,6} & 0 & 0 & 0 & 0 & 0 & 0 & 0 \\
0 & a_{6,2} & \frac{1}{L_{tr}} & 0 & a_{6,5} & -\frac{R_s}{L_{tr}} & 0 & 0 & 0 & 0 & 0 & 0 & 0 \\
0 & 0 & a_{7,3} & a_{7,4} & a_{7,5} & a_{7,6} & -\frac{1}{T_R} & 0 & 0 & 0 & 0 & 0 & 0 \\
0 & -\frac{K_D K_s}{2H} & a_{8,3} & a_{8,4} & a_{8,5} & a_{8,6} & 0 & -\frac{1}{T_W} & 0 & 0 & 0 & 0 & -\frac{K_s}{2H} \\
0 & -\frac{K_D K_s T_1}{2HT_2} & a_{9,3} & a_{9,4} & a_{9,5} & a_{9,6} & 0 & \frac{1}{T_2}(1 - \frac{T_1}{T_W}) & -\frac{1}{T_2} & 0 & 0 & 0 & -\frac{K_s T_1}{2HT_2} \\
0 & -\frac{K_D K_s T_1 T_3}{2HT_2 T_4} & a_{10,3} & a_{10,4} & a_{10,5} & a_{10,6} & 0 & T_3 - \frac{T_1 T_3}{T_W} & \frac{1}{T_4} - T_3 & -\frac{1}{T_4} & 0 & 0 & -\frac{K_s T_1 T_3}{2HT_2 T_4} \\
0 & \frac{K_I}{R} & 0 & 0 & 0 & 0 & 0 & 0 & 0 & 0 & 0 & 0 & 0 \\
0 & \frac{1}{RT_G} & 0 & 0 & 0 & 0 & 0 & 0 & 0 & 0 & \frac{1}{T_G} & -\frac{1}{T_G} & 0 \\
0 & 0 & 0 & 0 & 0 & 0 & 0 & 0 & 0 & 0 & 0 & \frac{1}{T_P} & -\frac{1}{T_P}
\end{bmatrix},
$$

$$B = E,$$

$$
C = \begin{bmatrix}
1 & 0 & 0 & 0 & 0 & 0 & 0 & 0 & 0 & 0 & 0 & 0 & 0 \\
0 & 0 & c_{2,3} & c_{2,4} & c_{2,5} & c_{2,6} & 0 & 0 & 0 & 0 & 0 & 0 & 0 \\
0 & 1 & 0 & 0 & 0 & 0 & 0 & 0 & 0 & 0 & 0 & 0 & 0 \\
0 & 0 & 0 & 0 & 0 & 0 & 0 & 0 & 0 & 1 & 0 & 0 & 0
\end{bmatrix},
$$

$$D = F,$$

where

$$
\begin{aligned}
a_{2,3} &= -\frac{I_{T,qo}}{2H} \\
a_{2,4} &= -\frac{I_{T,do}}{2H} \\
a_{2,5} &= -\frac{E'_{do}+(X'_q-X'_d)I_{T,qo})}{2H} \\
a_{2,6} &= -\frac{E'_{qo}+(X'_q-X'_d)I_{T,do})}{2H} \\
\\
a_{5,2} &= I_{T,qo} \\
a_{5,6} &= \frac{X'_q}{L_{tr}} + \omega_s + \Delta\omega_o \\
a_{6,2} &= -I_{T,do} \\
a_{6,5} &= -(\frac{X'_d}{L_{tr}} + \omega_s) - \Delta\omega_o \\
\\
a_{7,3} &= \frac{-R_s I_{T,qo} - X'_d I_{T,do} + E'_{qo}}{T_R\sqrt{(-R_s I_{T,do}+X'_q I_{T,qo}+E'_{do})^2+(-R_s I_{T,qo}-X'_d I_{T,do}+E'_{qo})^2}} \\
a_{7,4} &= \frac{-R_s I_{T,do} - X'_d I_{T,qo} + E'_{do}}{T_R\sqrt{(-R_s I_{T,do}+X'_q I_{T,qo}+E'_{do})^2+(-R_s I_{T,qo}-X'_d I_{T,do}+E'_{qo})^2}} \\
a_{7,5} &= \frac{-R_s(-R_s I_{T,do}+X'_q I_{T,qo}+E'_{do})-X'_d(-R_s I_{T,qo}-X'_d I_{T,do}+E'_{qo})}{T_R\sqrt{(-R_s I_{T,do}+X'_q I_{T,qo}+E'_{do})^2+(-R_s I_{T,qo}-X'_d I_{T,do}+E'_{qo})^2}} \\
a_{7,6} &= \frac{X'_q(-R_s I_{T,do}+X'_q I_{T,qo}+E'_{do})-R_s(-R_s I_{T,qo}-X'_d I_{T,do}+E'_{qo})}{T_R\sqrt{(-R_s I_{T,do}+X'_q I_{T,qo}+E'_{do})^2+(-R_s I_{T,qo}-X'_d I_{T,do}+E'_{qo})^2}} \\
\\
a_{8,3} &= -\frac{K_s I_{T,qo}}{2H} \\
a_{8,4} &= -\frac{K_s I_{T,do}}{2H} \\
a_{8,5} &= -\frac{K_s(E'_{do}+(X'_q-X'_d)I_{T,qo})}{2H} \\
a_{8,6} &= -\frac{K_s(E'_{qo}+(X'_q-X'_d)I_{T,do})}{2H} \\
\\
a_{9,3} &= -\frac{K_s T_1 I_{T,qo}}{2HT_2} \\
a_{9,4} &= -\frac{K_s T_1 I_{T,do}}{2HT_2} \\
a_{9,5} &= -\frac{K_s T_1(E'_{do}+(X'_q-X'_d)I_{T,qo})}{2HT_2} \\
a_{9,6} &= -\frac{K_s T_1(E'_{qo}+(X'_q-X'_d)I_{T,do})}{2HT_2}
\end{aligned}
$$

$$
\begin{aligned}
a_{10,3} &= -\frac{K_s T_1 T_3 I_{T,qo}}{2HT_2T_4} \\
a_{10,4} &= -\frac{K_s T_1 T_3 I_{T,do}}{2HT_2T_4} \\
a_{10,4} &= -\frac{K_s T_1 T_3 (E'_{do}+(X'_q-X'_d)I_{T,qo})}{2HT_2T_4} \\
a_{10,5} &= -\frac{K_s T_1 T_3 (E'_{qo}+(X'_q-X'_d)I_{T,do})}{2HT_2T_4}
\end{aligned}
$$

$$
\begin{aligned}
c_{2,3} &= \frac{-R_s I_{T,qo}-X'_d I_{T,do}+E'_{qo}}{\sqrt{(-R_s I_{T,do}+X'_q I_{T,qo}+E'_{do})^2+(-R_s I_{T,qo}-X'_d I_{T,do}+E'_{qo})^2}} \\
c_{2,4} &= \frac{-R_s I_{T,do}-X'_d I_{T,qo}+E'_{do}}{\sqrt{(-R_s I_{T,do}+X'_q I_{T,qo}+E'_{do})^2+(-R_s I_{T,qo}-X'_d I_{T,do}+E'_{qo})^2}} \\
c_{2,5} &= \frac{-R_s(-R_s I_{T,do}+X'_q I_{T,qo}+E'_{do})-X'_d(-R_s I_{T,qo}-X'_d I_{T,do}+E'_{qo})}{\sqrt{(-R_s I_{T,do}+X'_q I_{T,qo}+E'_{do})^2+(-R_s I_{T,qo}-X'_d I_{T,do}+E'_{qo})^2}} \\
c_{2,6} &= \frac{X'_q(-R_s I_{T,do}+X'_q I_{T,qo}+E'_{do})-R_s(-R_s I_{T,qo}-X'_d I_{T,do}+E'_{qo})}{\sqrt{(-R_s I_{T,do}+X'_q I_{T,qo}+E'_{do})^2+(-R_s I_{T,qo}-X'_d I_{T,do}+E'_{qo})^2}}.
\end{aligned}
$$

BIOGRAPHY

Born in Bangkok, Thailand, in 1985, Kittichai Tia obtained his Bachelor degree in electrical engineering from Chulalongkorn University, Thailand, in 2007. He was granted Chulalongkorn University Scholarship of the Honor Graduate Program for Electrical Engineering Students to pursue his Master's degree in electrical engineering at Chulalongkorn University, Thailand during 2007–2008. He studied, did his research and served on the teaching assistant at Control Systems Research Laboratory, Department of Electrical Engineering, Faculty of Engineering, Chulalongkorn University, Thailand.

Throughout the undergraduate and graduate studies, his research was under the supervision of Assistant Professor Suchin Arunsawatwong. His field of interest includes power system stability and control, computer aided design of control systems. During the Master's program, he has published a research work entitled "Design of Compensators for Power Systems Operating under Load Voltage Fluctuation Satisfying Bounding Conditions" in the proceedings of the Electrical Engineering/Electronics, Computer, Telecomunications and Information Technology (ECTI) Conference 2009, Thailand.

He was granted a visiting scholarship by Toshiba International Foundation to enroll in a hands-on training program at the Power and Industrial System Reserarch and Development Center, Toshiba Corporation, Tokyo, Japan for three months in spring 2009 after his Master's graduation.